Mechanisms underlying diverse short-term plasticity of thalamocortical synaptic responses in the whisker system

Giovanni Ferrati

2015

Tutor of the PhD thesis: Miguel Maravall

Instituto de Neurociencias de Alicante

Universidad Miguel Hernández - CSIC

Contents

List of abbreviations

8-CPT: 8-Cyclopentyl-1,3-dimethylxanthine

A1R: adenosine receptor group 1

ACET: (*S*)-1-(2-Amino-2-carboxyethyl)-3-(2-carboxy-5-phenylthiophene-3-yl-methyl)-5-methylpyrimidine-2,4-dione

ACSF: artificial cerebro-spinal fluid

AMPAr: α-amino-3-hydroxy-5-methyl-4-isoxazolepropionic acid receptor

ATP: adenosine-5'-triphosphate

BC: barrel cortex

CF: climbing fibre

CTX: cortex

D-APV: D-(-)-2-Amino-5-phosphonopentanoic acid

DIC: differential interference contrast microscopy

DNDS: dinitrostilbene-2,2'-disulfonic acid

DPCPX: 8-Cyclopentyl-1,3-dipropylxanthine

EPSCs: excitatory postsynaptic currents

FI: facilitation index

FS: fast spiking neurons

GABA: γ-Aminobutyric acid

H: hippocampus

INs: interneurons

IPSCs: inhibitory postsynaptic currents

ISIs: interstimulus intervals

LTP: long-term plasticity

MCx: primary motor cortex

NMDAr: N-methyl-D-aspartate receptor

NS-102: 6,7,8,9-Tetrahydro-5-nitro-1H-benz[g]indole-2,3-dione 3-oxime

PF: parallel fibre

POm: posteromedial nucleus

P_r: probability of transmitter release

PrV: principal trigeminal nucleus

PSP: post synaptic potential

RS-(CPP): (*RS*)-3-(2-Carboxypiperazin-4-yl)-propyl-1-phosphonic acid

RS: regular spiking neurons

S1: primary somatosensory cortex

S2: secondary somatosensory cortex

SC: Schaffer collateral

SpV: spinal trigeminal nucleus

SpVc: spinal trigeminal nucleus caudalis

SpVi: spinal trigeminal nucleus interpolaris

SpVir: spinal trigeminal nucleus interpolaris, rostral part

SpVo: spinal trigeminal nucleus oralis

STP: short-term plasticity

Str: striatum

TC: thalamocortical

TCS: Tuning curve slope

Th: thalamus

TN: trigeminal nuclei

UBP 296: (*RS*)-1-(2-Amino-2-carboxyethyl)-3-(2-carboxybenzyl)pyrimidine-2,4-dione

UBP 310: (*S*)-1-(2-Amino-2-carboxyethyl)-3-(2-carboxy-thiophene-3-yl-methyl)-5-methylpyrimidine-2,4-dione

VB: ventrobasal

VPMc: ventral posterior medial cells placed at the core of the barreloids

VPMdm: ventral posterior medial nucleus, dorsomedial part

VPMh: ventral posterior medial cells placed at the head of the barreloids

VPMvl: ventral posterior medial nucleus, ventrolateral part

ZI: Zona Incerta

List of figures

Summary

Mechanisms underlying diverse short-term plasticity of thalamocortical synaptic responses in the whisker system

In the somatosensory system, thalamocortical (TC) projections are responsible for transmitting sensory stimuli to the cortex and are thus crucial to the perception of sensory stimuli (Bruno, Sakmann, 2006). In the rodent neocortex, layer 4 neurons are the main target of lemniscal thalamic drive via monosynaptic connections. Consequently, the modulation of the dynamics of TC connections onto layer 4 plays a fundamental role in the transmission and processing of sensory information from the external environment. Excitatory connections to layer 4 have been historically described as depressing both *in vitro* (Gil et al., 1997, 1999; Stratford et al., 1996) and *in vivo* (Chung et al., 2002; Bruno, Sakmann, 2006). Classic studies were designed to evaluate the depressing effect on TC connections of a periodic stimulation starting from rest. However, this paradigm does not reflect the richness of stimuli received at individual synaptic connections under physiological conditions. In living animals, external stimuli arrive to the cortex together with a complex and rich background of spontaneous and evoked activity, which may affect different connections in distinct ways. Therefore, synaptic plasticity should not be described only in terms of periodic stimulation from rest, or according to the average properties of populations of a given type.

In order to examine short-term plasticity (STP) dynamics of TC synapses, we measured whole-cell responses to stimulation of TC fibers in layer 4 neurons, using a mouse barrel cortex slice preparation. Previous results from our group (Diaz-Quesada, Martini et al., 2014) showed that STP is variable across TC synapses when evaluated with ongoing, naturalistic stimulation. Consistent with classic earlier work TC connections stimulated from rest (silence) with a regular pattern were characterized by depressing behavior. In contrast, a much more diverse synaptic behavior was found across TC connections when recorded during ongoing stimulation. Each connection responded differentially to particular stimulation intervals, enriching the ability of the pathway to convey complex, temporally fluctuating information. In particular, a change from periodic stimulation to an irregular pattern consisting of different interstimulus intervals (ISIs) yet with identical average frequency (4.59 Hz) unveiled synaptic responses that could be dominated either by facilitation or depression.

In the present work we have tried to find principles governing this diversity of STP in the TC pathway, focusing on two main factors: the mechanisms underlying STP heterogeneity and the possible rules for specificity across synapses connecting to a single specific neuron. Our results suggest that diverse plasticity is not a consequence of a variable amount of inhibition but occurs across the population of monosynaptic excitatory TC connections. We confirmed that NMDA receptor blockade had no effect on the distribution of STP, but extracellular calcium concentration did, supporting a dependence on presynaptic mechanisms. Therefore we aimed our attention at two presynaptic mechanisms that can regulate release probability and consequently short-term plasticity. First, we analyzed adenosine receptors (A1R): recordings in the presence of adenosine and its antagonist DPCPX and 8-CPT evidenced that perturbing the action of A1R modifies the release probability and short-term plasticity of TC synapses. Specifically, applying adenosine increased facilitation while applying DPCPX enhanced depression. However, these manipulations did not eliminate variability across synapses, suggesting that there is underlying variability in the expression of the machinery for calcium entry and neurotransmitter release. We also examined kainate receptors (KARs), which display age-dependent presynaptic expression in TC synapses and may regulate release probability. We explored possible roles for kainate receptors in short-term plasticity by altering KAR expression both pharmacologically and via the use of knockout mice. We found no evidence for a modulatory effect of KARs on TC short-term plasticity. Finally, concerning specificity, we designed a strategy aimed to find a regulation at the cell level. Our experiments provided weak evidence for postsynaptic clustering of STP properties.

1. Introduction

Animals live in a dynamic environment where they constantly receive stimuli that unfold in time and space. In the somatosensory, visual and auditory system sensory information is relayed to the cortex through the thalamus. Therefore analyzing the dynamics of thalamocortical (TC) synapses is necessary to understand how sensory information arrives and is processed in the cortex.

1.1 The somatosensory system

In common with other sensory modalities, the somatosensory system – including receptors, transmitting elements and processing centers – reacts to diverse stimuli received at the periphery and transmitted afterwards to higher processing areas in order to produce a specific response. It consists of a number of different receptors, including thermoreceptors, proprioceptors, mechanoreceptors and nociceptors. It informs us about objects in our external environment through touch and about the position and movement of our body parts (proprioception) through the stimulation of muscle and joints. The somatosensory system also monitors the temperature of the body, external objects and environment, and provides information about painful, itchy and tickling stimuli.
Somatosensory information travels along different anatomical pathways depending on the information carried. In rodents, the barrel cortex is a specialized region of the somatosensory system responsible for processing information from whiskers. The whisker system is a fundamental channel for collecting tactile information from the environment. Since they are animals living much of the time underground, this system plays a major role in their exploration both for identifying the location of objects and their properties and identity (Diamond et al., 2008).

1.1.1 The rodent somatosensory system: pathways and somatotopy

The rodent somatosensory system is characterized by a well-defined somatotopic map where each individual whisker is represented at the cortical level in a discrete

anatomical unit, the "barrel", allowing precise delineation of functional organization, development, and plasticity (Fig. 1.1). In rodents somatotopy is maintained along the principal (lemniscal) sensory pathway, giving rise to "barreloids" at thalamic level and "barrelettes" in the brainstem.

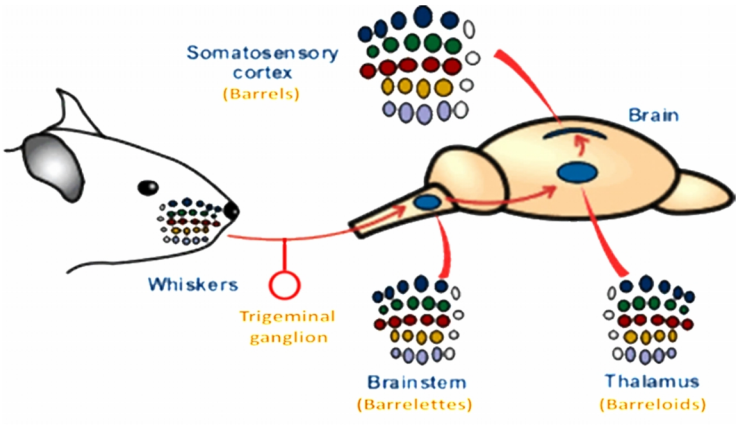

Figure 1.1: Anatomical somatotopy.
Schematic representation of the somatotopic organization of the whisker to barrel pathway. Barrel cortex contains an orderly map which corresponds with the arrangement of the facial whiskers. This somatotopy is maintained in the barrelettes in the brainstem and in the barreloids in the thalamus.

The deflection of a whisker opens mechano-gated ion channels in nerve endings of first order sensory neurons innervating the hair follicle. The resulting depolarization evokes action potential firing in sensory neurons of the infraorbital peripheral branch of the trigeminal ganglion. About 200 first order cells of the trigeminal ganglion per whisker send in addition a central branch to the Trigeminal Nuclei (TN) complex in the brainstem. The brainstem TN complex represents the first processing stage in the vibrissal system. It comprises the principal trigeminal nucleus (PrV) and the spinal trigeminal nucleus (SpV), which consists of the oralis (SpVo), interpolaris (SpVi) and caudalis (SpVc) subnuclei. In the PrV cells are organized in barrelettes each of which is connected to a single whisker. The TN sends afferents to the thalamus through 4 different pathways (Fig. 1.2A,B):

- Lemniscal (1) pathway: neurons organized in barrelettes in the PrV of the brainstem send axons to the contralateral part of the dorsomedial section of the Ventral Posterior Medial nucleus (VPMdm) of the thalamus through the lemniscal pathway. In this area a single type of neuron, termed relay cells, are clustered in whisker-related structures called barreloids receiving vibrissal input

principally from small-sized PrV neurons whose receptive field is dominated by a single whisker. Third order neurons from the VPMdm connect to the primary somatosensory cortex where they terminate in barrels, a dense group of cells in layer 4.

- Lemniscal (2) pathway: at the dorsomedial margin of the VPM, near the thalamic posterior medial nucleus (Pom), there is a stratum of barreloid cells that receive vibrissal input from an additional population of PrV cells with large multiwhisker receptive fields (Veinante, Deschênes, 1999). In contrast with VPM cells placed at the core of the barreloids (VPMc) whose receptive field is dominated by a single vibrissa, those situated in the head of the barreloids (VPMh) respond equally well to multiple vibrissae (Urbain, Deschênes, 2007). Although cortical targets for this pathway still need to be studied, there are clues suggesting that VPMh cells project principally to septal regions.
- Extralemniscal pathway: the neurons placed in the caudal part of the SpVi project to the VentroLateral part of the VPM (VPMvl). VPMvl thalamic cells exhibit large multiwhisker receptive fields that are independent of input from the PrV. Here cells are not clearly recognizable with immunohistochemical stain but they are clustered into the 'tails' of the VPMdm barreloids. The axons of VPMvl neurons project to the septa between the barrels of S1 and to the secondary somatosensory cortex (S2).
- Paralemniscal pathway: the multiwhisker cells located in the rostral part of the SpVi (SpVir) contact the posteromedial nucleus (POm) in the thalamus and the Zona Incerta (ZI); third order neurons from the POm send afferents to layer 5a just below the barrels, to layer 1 and to S2 and the primary motor cortex (MCx).

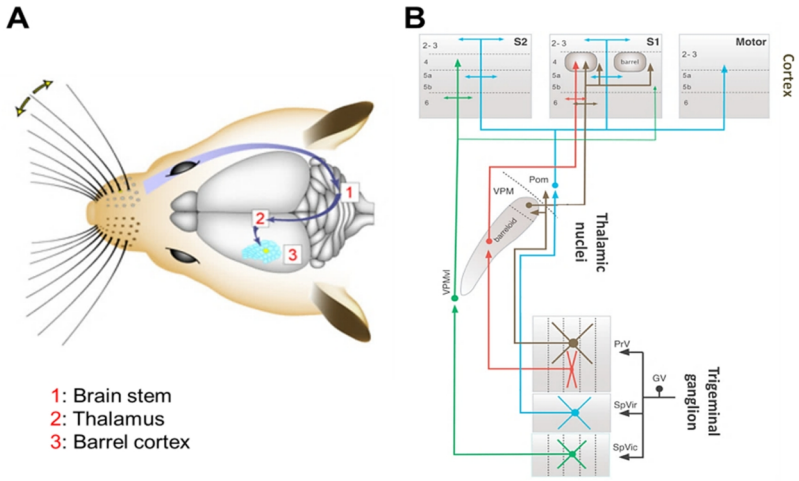

Figure 1.2: Pathway from the whiskers to the cortex.

Sensory information flows in parallel pathways from whiskers to cortex. **A**, Picture indicating the three main stations of the pathway from the whiskers to the cortex. Modified from (Petersen, 2007). **B**, Anatomical organization of the pathways. Red line: lemniscal (1) pathway, brown line: lemniscal (2) pathway, green line: extralemniscal pathway, blue line: paralemniscal pathway. Modified from (Deschenes, Urbain, 2009).

At the cortical level, the layer 4 barrel map replicates the organization of the whiskers on the snout (Woolsey, Van der Loos, 1970), where large whiskers (or macrovibrissae) are arranged in a grid with five rows (from A to E) along the antero-posterior axis and several arcs placed orthogonally (Fig. 1.3). Even though neurons in the barrel cortex have a receptive field that extends to several whiskers, the topographic organization makes neurons in the barrel cortex and the thalamus respond preferentially to stimulation of one whisker and weakly to several adjacent. The whisker associated to the strongest response in each column is known as the "principal whisker". Each barrel column is composed of neurons that show a preferential response to the deflection of the whisker corresponding to that barrel (Welker, 1976; Simons, 1978).

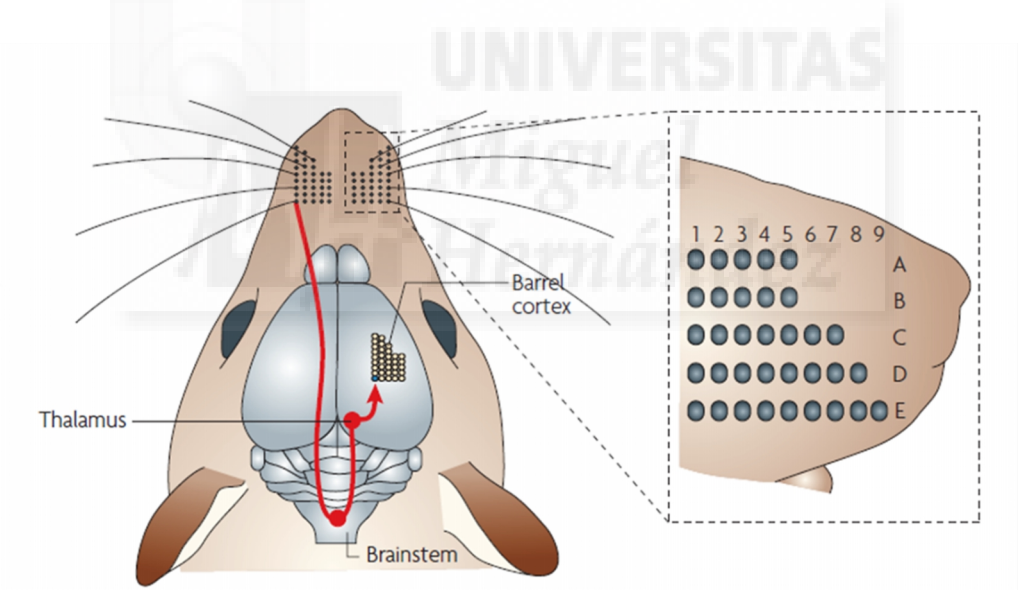

Figure 1.3: Whisker arrangement.
The vibrissae form a two-dimensional grid of five rows designated from A to E on each side of the snout. Each row contains from five to nine whiskers. Information from a single whisker (E1 in the picture) reaches the brainstem where axons of the second-order neurons cross the midline and travel to the thalamic nuclei; thalamic neurons project to the corresponding barrel in the primary somatosensory cortex. Modified from (Diamond et al., 2008).

1.1.2 The rodent somatosensory system: active whisking

Rodent whiskers are moveable tactile (touch) sensors, loosely similar to human fingertips. Rodents collect sensory information from the environment through their whiskers, including bilateral, 5–12 Hz ‘‘exploratory’’ forward and backwards movements by macrovibrissae - the long (3 to 40 mm) whiskers located on the middle and posterior part of a rat’s snout - and slower passage of both macrovibrissae and microvibrissae - shorter whiskers clustered anteriorly on the snout - across objects by head motion (Jadhav, Feldman, 2010). To make behavioral choices, rodents need to identify the shape and texture of objects whisking actively with macrovibrissae and touching passively the surfaces with the microvibrissae, characterized by little or no whisking motion. Thanks to this structural organization of the whisker system, rodents sense external stimuli and can acquire information about object position and shape, surface properties and ultimately object identity. In the whisker sensorimotor system the sensory and motor components are intimately interconnected and reciprocally influenced in order to collect significant information, with motor output generating sensory input, sensory input modulating motor output. Recent data show that rodents can either generate sensations or receive sensations. There are two possible modes in which whisker-mediated sensation can occur (Maravall, Diamond, 2014): in the generative mode, the animal moves its whiskers to actively seek contact with objects and palpate them, while in the receptive mode the animal places its whiskers on an object and is frequently observed to immobilize its whiskers to optimize signal collection. Many different tasks have been designed involving the generative mode such as wall following (Jenks et al., 2010), gap measurement (Hutson, Masterton, 1986), texture discrimination (Zuo et al, 2011), and object localization (Knutsen, Ahissar, 2011). Tasks involving the receptive mode include detection and discrimination of vibrations applied to whiskers (Hutson, Masterton, 1986), and discrimination of the width of an aperture (Krupa et al., 2001). It has been proposed (Diamond et al., 2008) that rodents are able to distinguish two major types of information processed in different specific neural pathways: first, the location of objects in the environment, relative to the animal’s head position (‘where’), conveyed by the extralemniscal pathway, and second, the properties and identity of objects (‘what’), conveyed by the lemniscal pathway (Yu et al., 2006).

1.1.3 The somatosensory cortex: cellular and synaptic organization

In mammals the neocortex represents the majority of the mammalian brain and is involved in higher functions such as sensory perception, generation of motor commands, spatial reasoning, behavior and cognition. It is made up of six layers, labelled from the outer in, 1 to 6. Neurons of the neocortex are arranged in vertical structures called cortical columns. Each column typically responds to a sensory stimulus arriving at different sensory cortical areas and representing certain body part or region of sound or vision. These columns process incoming inputs similarly, and therefore can be considered as the basic repeating functional units of the neocortex.

Neurons in the neocortex contain two primary types of neurons, excitatory glutamatergic neurons (~80% of neocortical neurons) and inhibitory GABAergic interneurons (~20%).

There are numerous subtypes of inhibitor neurons in the neocortex, each of which shows differences in axonal arbors, soma, dendritic morphology, secondary neuropeptide transmitter produced and intrinsic membrane properties. In common they have GABA as a primary neurotransmitter. A useful classification is based on the area where they form synapses on target cells. Following this criterion we can recognize soma-targeting cells (including basket cells), axon-targeting cells (including chandelier cells), dendrite-targeting cells (including double bouquet cells, bitufted cells, and bipolar cells) and other categories such as Martinotti cells and Cajal-Retzius cells.

There are three main types of excitatory neurons in the neocortex: the spiny stellate, the star pyramid and the pyramidal cell. Spiny stellate cells are characterized by a star-shaped dendritic pattern. Most spiny stellate cells are located in layer 4 of the somatosensory cortex, with dendrites oriented towards the center of the barrel and axons running mainly in a columnar orientation toward layer 1 with arborization in layer 2, 3 and 4. They also project down toward layer 5 and 6 (Lubke et al., 2000). Approximately 20-25% of the cells in layer 4 of rat barrel cortex are star pyramids. They have a short ascending main apical dendrite that doesn't reach layer 1. The basal dendrites are symmetrical while axons project to layers 2/3 and 4, with a few branches reaching layer 5/6. Pyramidal neurons have a triangular soma and typically a single axon and multiple basal dendrites. They are located across the cortical layers and are characterized by one main apical dendrite extending through the layers above their soma. In cortical layer 4, neurons receive numerous synaptic connections from outside the cortex (mostly from

thalamus) and make short-range, local connections to other cortical layers. Thus, layer 4 receives incoming sensory information and distributes it to the other layers for further processing.

In the somatosensory cortex we can also differentiate neurons according to their response to somatic current injection. There are three main electrophysiologically defined types of neurons in layer 4: regular-spiking (RS) cells show spike accommodation and include most excitatory cells such as spiny stellate neurons or pyramidal neurons (Fig. 1.4).

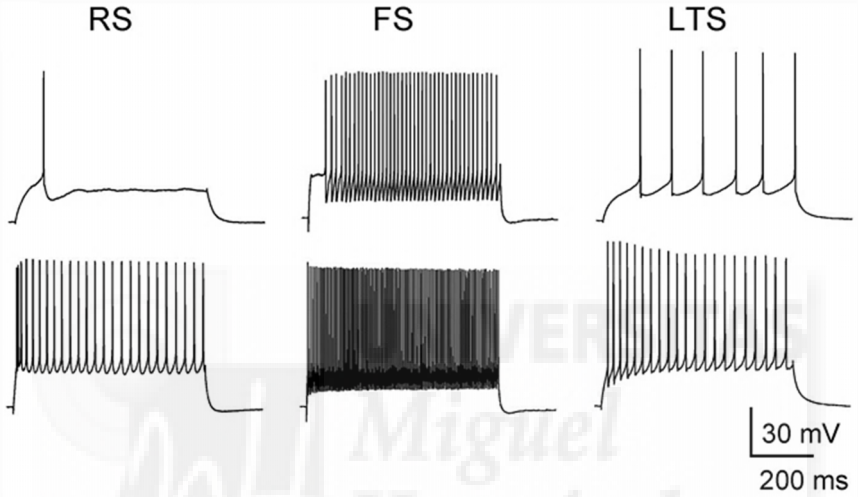

Figure 1.4: Firing patterns of cortical neurons.
Intrinsic firing pattern of 3 types of layer 4 neurons. Depolarizing current steps evoke low-frequency firing in RS and LTS cells at threshold, whereas FS neurons display high minimum firing frequencies. Current steps at higher amplitudes evoke spike-frequency adaptation in RS and LTS cells but not in FS cells. Modified from (Beierlein et al., 2003).

Fast spiking (FS) cells respond to current injection with action potentials of short duration and without decreasing the frequency. This firing pattern is typical of inhibitory neurons. Low-threshold-spiking (LTS) neurons have a particularly low threshold for evoking action potentials due to activation of a low threshold calcium current. This pattern is characteristic of inhibitory bitufted neurons.

1.1.4 Spatio-temporal information dynamics in the whisker sensorimotor system

In natural conditions, relevant external stimuli evoking behavioral responses are made of patterns that vary over time and are sensed peripherally and processed centrally in the

higher cortices. Examples are bird vocalizations emitted as a series of sounds processed in the auditory system or the vibrations perceived by skin mechanoceptors in touch. In the somatosensory cortex, the movements of whiskers exploring the position of objects or the texture of surfaces are characterized by high-velocity micromotions, termed whisker slips and sticks, at irregular intervals (Jadhav, Feldman, 2010). Sensory information that varies over time is encoded and modulated at central synapses along the pathway depending not just on stimulus features, but also on synaptic properties and state of activation.

Sensory input to layer 4 neurons is mediated by monosynaptic connections from the thalamus. Alone, TC projections, a small but powerful set of axons, account for just about 15% of synapses onto cortical neurons but they represent the principal input from the outside environment (Benshalom, White, 1986). Modifications in the properties of TC connections can shape the dynamics of information transmission from the periphery to central processing areas. Therefore, elucidating the mechanisms responsible for synaptic plasticity at TC connections is necessary to understand how sensory stimuli from the surrounding environment are translated into neuronal spike trains able to determine behaviorally relevant responses.

1.2 Information dynamics in cortical networks: brain plasticity

Synaptic communication is a highly adaptive process dynamically modulated by local adjustments of synaptic efficacy. Efficacy can change after the onset of specific temporal patterns of activity, either increasing (synaptic facilitation) or decreasing (synaptic depression), over time scales that can range from milliseconds to months. Synaptic connections are thus dynamic entities whose effect on the postsynaptic neuron can strengthen or weaken over time, depending on their history of usage and prior activity (Abbott, Regehr, 2004). This intrinsic capacity to vary the behavior – synaptic plasticity – can be divided into two major categories depending on the duration of its effects on the synapse: long-term plasticity (LTP), involving changes lasting for hours or longer, is believed to be the major cellular mechanism underlying learning and memory (Bliss, Collingridge, 1996), while short-term plasticity (STP), involving changes lasting from tens of milliseconds to a few minutes, is a phenomenon in which

synaptic efficacy changes over a short period of time in a way that reflects the history of synaptic activation.

1.2.1 Short-term synaptic plasticity

STP can be defined as the effect of activity on instantaneous changes in synaptic efficacy, occurring in a range of milliseconds to minutes. The history of synaptic activity can modulate those changes to give rise to different types of plasticity that either facilitate (Short-term facilitation, STF) or depress (Short-term depression, STD) the response, leading consequently to the alteration of neural information transmission (Abbott et al. 1997; Tsodyks, Markram, 1997). Synapses transmit information when presynaptic action potentials are able to cause the fusion of vesicles containing diverse neurotransmitters to the presynaptic membrane, thus releasing neurotransmitter. Neurotransmitter release thus depends on presynaptic activity which is determined by the response to afferent stimuli, each of which is characterized by a peculiar spatio-temporal structure. Every neuron in the nervous system may receive synaptic inputs from thousands of other neurons. A postsynaptic threshold is reached, and an action potential generated, only if the spatial inputs arriving from multiple neurons or temporal inputs from a single neuron, or both, summate at a given moment. This allows the postsynaptic neuron to be sensitive to spatial and temporal properties of incoming information, making cortical networks inherently capable of processing complex spatio-temporal stimuli.

Different categories of synaptic connections in different areas can have varied forms of plasticity, ranging from facilitating to depressing, including a combination of both. Synapses show a wide range of responses to high-frequency stimulation and STP is a reflection of changes in the probability of vesicle release. Although postsynaptic processes can participate in changes in synaptic strength, to understand the mechanisms underlying STP, it is necessary to consider presynaptic processes. Facilitation seems to be due to an increase in the mean number of quanta of transmitter from the presynaptic terminal; with repetitive stimulation accumulation of residual calcium leads to a progressive increase in transmitter release. In contrast, depression may be associated with both depletion of quanta and reduced release efficacy due to a reduction in calcium influx. The probability of transmitter release (p_r) upon a single presynaptic spike differs

markedly across synapses. Depression generally occurs at 'high- p_r' synapses, whereas facilitation is prominent at 'low- p_r' synapses.

Example of synapses with high initial release probabilities are the cerebellar climbing fiber to Purkinje cells synapses, which depress quickly and operate as low-pass filters, responding to lower-frequency signals (Fig. 1.5A,B). At facilitating synapses, release probability is small and only minimally decreased by the first few spikes. If the frequency is sufficiently high, residual Ca^{2+} could build up in the terminal, thereby facilitating transmitter release. Synapses with a low initial probability of vesicle release are represented by parallel fiber to Purkinje cells synapses in the cerebellum, which tend to facilitate with repeated use and thus act as high-pass filters. Synapses with an intermediate probability of release, such as Schaffer collateral synapses in the hippocampus, act as band-pass filters that selectively respond to a specific range of frequencies (Abbott, Regehr, 2004). In general, STD-dominated synapses allow information transfer for low firing rates, since high-frequency spikes rapidly deactivate the synapse.

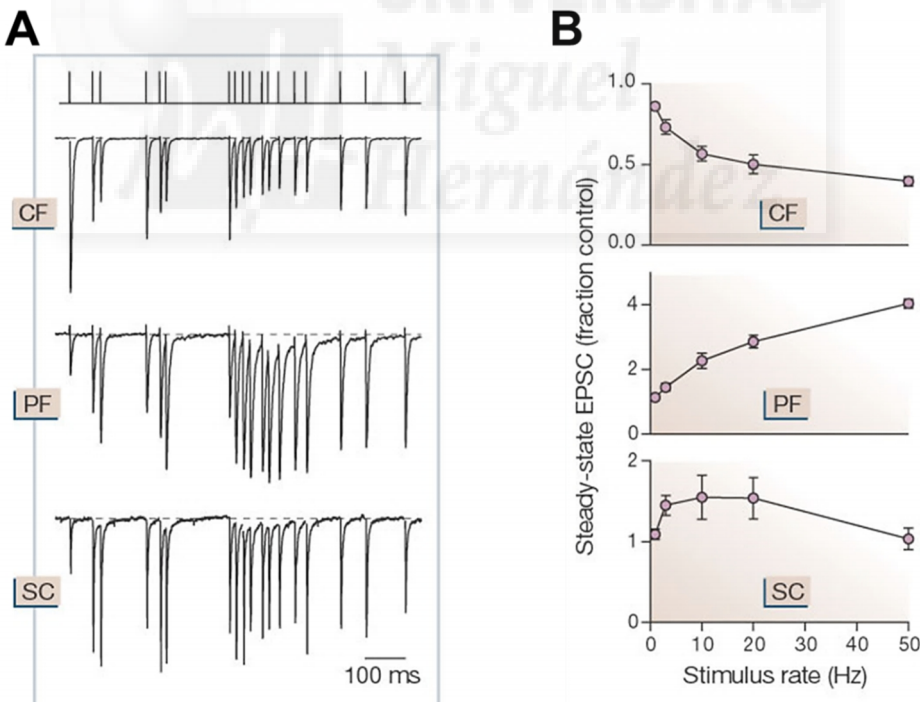

Figure 1.5: Diversity of short-term dynamics.
A, Excitatory postsynaptic currents (EPSCs) recorded in response to an irregular stimulus train with an average rate of 20 Hz at three different synaptic connections: the climbing fibre (CF), parallel fibre (PF) and Schaffer collateral (SC) synapses. Diversity of short-term plasticity between the three different connections: top, climbing fibre to Purkinje cell EPSCs; middle, parallel fibre to Purkinje cell EPSCs; bottom, CA3 to CA1 Schaffer collateral EPSCs. Traces are averages of four to six trials. **B**, Average magnitude of the eighth to tenth EPSC from a

regular train, normalized by the first EPSC and plotted as a function of stimulus frequency for CF (top), PF (middle) and SC (bottom) synapses. Modified from (Abbott, Regehr, 2004).

STP exhibits great diversity in properties even for synapses connecting neurons of the same class (Dittman et al. 2000). Experiments of triple and quadruple neuron recordings revealed that each synaptic connection established by neocortical pyramidal neurons is potentially unique (Markram et al. 1996). More specifically, paired pyramidal targets of the same morphological and electrophysiological classes show different degrees of synaptic depression when contacted by the same presynaptic axon. Heterogeneity of synaptic properties also occurs when convergent inputs of the same morphological class (pyramidal neurons) contact a postsynaptic interneuron.

1.2.2 Pre- and post-synaptic factors modulating STP

A number of different factors have been shown to mediate STP, each of which is ascribable to two main categories, presynaptic and postsynaptic.

1.2.2.1 Presynaptic factors

As already mentioned, synaptic efficacy can increase (synaptic facilitation) or decrease (synaptic depression) within milliseconds after the onset of specific temporal patterns of activity. Following a simple biophysical model (Markram et al., 1998; Gil et al., 1999) the mean efficacy of a synaptic connection between two neurons (E) can be defined as the synaptic response generated by any action potential when activated by a stimulus. E is determined by three parameters, such that $E = q \cdot n \cdot p_r$, where q is the mean quantal size, n is the number of release sites of a presynaptic axon contacting its postsynaptic targets, and p_r is the mean probability of neurotransmitter release at each site. The parameter q refers to the amplitude of the postsynaptic response to a single synaptic vesicle (Katz, 1969). Neurotransmitters are released in a small package called quantum; each quantum evokes a stereotyped post-synaptic response. Diverse synaptic connections could show different quanta release thus explaining the variability in synaptic efficacy. The parameter n is determined by the number of release site contacts

between the presynaptic axon and the post-synaptic neuron; it is variable depending on brain area and connection type. An increase in the number of synaptic contacts is associated with a stronger response to presynaptic inputs. The parameter p_r depends on the cellular mechanisms underlying neurotransmission at synaptic sites. Periods of elevated presynaptic activity can cause either an increase or a decrease in neurotransmitter release. Short-term synaptic enhancement reflects an increase in the probability of release of available quanta (Abbott, Regehr, 2004). Facilitation is associated to an increase in the probability of neurotransmitter release. Conversely, depression reflects a decrease in the probability of neurotransmitter release per synapse. In most synapses there is a combination of facilitatory and depressing dynamics, with their relative weight depending largely on the initial probability (Abbott, Regehr, 2004; Dittman et al., 2000).

1.2.2.2 Postsynaptic factors

Together with the presynaptic factors, the postsynaptic partners can participate in STP diversity and cooperate to modulate the underlying mechanisms. Target cell specific forms of plasticity imply that postsynaptic cells must signal across the synapse to the presynaptic terminal to determine its properties. STP can be directly postsynaptically determined: it has been demonstrated that saturation of postsynaptic receptors can accelerate recovery from depression (Foster et al., 2002). Postsynaptic receptors can undergo desensitization when exposed to neurotransmitter following the first action potential. This causes them to enter a nonconducting, desensitized state during which they cannot be responsive (Xu-Friedman, Regehr, 2004).

Moreover, postsynaptic cells are able to regulate specifically their own presynaptic compartment by retrograde signaling without affecting neighboring presynaptic compartments. Several retrograde messengers such as nitric oxide and endocannabinoids seem to influence the regulation of the release of neurotransmitter and a number of synaptic adhesion molecules enable specific retrograde regulation of presynaptic compartments (Blackman et al., 2013; Bozdagi et al., 2004; Dean, Dresbach, 2006).

1.2.3 Neuromodulators effect on STP

Synaptic communication between neurons is under a fine modulatory control. Neurotransmitters released from a presynaptic neuron bind to specific ionotropic receptors that allow the flow of specific ions across the postsynaptic cell membrane causing an immediate effect. However, synaptic terminals in the central nervous system possess high-affinity metabotropic receptors that can be activated by chemical messengers called neuromodulators. Neuromodulators act on metabotropic receptors regulating the activity of synapses in a facilitating or depressing manner, causing effects that can persist from several hundred milliseconds to several hours. It has been thoroughly demonstrated that metabotropic receptors are linked to various signal transduction mechanisms via G-proteins. The binding of neurotransmitters to metabotropic receptors in the postsynaptic cell initiates a cascade of biochemical events involving intracellular molecules called second messengers. Although the neurotransmitter, or "first messenger", becomes inactivated rapidly, the effects of the second messenger may last much longer. After the release, neuromodulators can act either homosynaptically and bind to presynaptic autoreceptors or heterosynaptically by diffusing to nearby terminals (Zucker, Regehr, 2002).

1.2.3.1 Homosynaptic modulation

The content of the vesicles liberated from the presynaptic cell can act on presynaptic autoreceptors exerting a homosynaptic modulation. A few modulators involved in this kind of process will be described here. Inside the family of neuromodulators that have been analyzed, adenosine has a mechanism of action that has been extensively studied and can participate as a homosynaptic regulator. Vesicles contain ATP at high concentration. Following vesicle exocytosis, ATP is released in the extracellular space and degraded to adenosine. Adenosine activates presynaptic metabotropic receptors and determines a homosynaptic inhibition of transmitter release by reducing presynaptic Ca^{2+} influx through activation of A1 receptors (Gundlfinger et al., 2007). In another example, in rat hippocampus, some GABAergic synapses (Davies et al., 1990) show depression due to a retrograde action of GABA on presynaptic $GABA_B$ metabotropic receptors, presumably reducing Ca^{2+} influx by modulating voltage gated Ca^{2+} channels.

In addition to forming ion channel pores as ionotropic glutamate receptors (iGluR), including NMDA, AMPA and kainate family, glutamate receptors can have metabotropic activity following activation of a specific family, the metabotropic glutamate receptors (mGluR). They indirectly activate ion channels on the plasma membrane through a signaling cascade that involves G-proteins. A further metabotropic pathway is mediated by kainate receptors. The classic signaling pathway of these receptors has been extensively studied. Kainate ionotropic receptors are responsible in the hippocampus for mediating neurotransmission by bidirectional regulation of glutamate release depending on its concentration. Interestingly, it has been demonstrated that kainate receptors can also act through a non-canonical signaling pathway involving the initiation of a second-messenger cascade following the activation of a G-protein coupled to the receptor (Frerking, et al., 2001). It has been proposed that presynaptic kainate receptors in Schaffer collaterals could inhibit Ca^{2+} channels via the non-canonical pathway resulting in the inhibition of transmitter release and modulation of postsynaptic parameters (Lerma, 2003).

1.2.3.2 Heterosynaptic modulation

Presynaptic terminals exhibit receptors for transmitters that are released from other neighboring neurons, and activation of these can also influence the release process. Such receptors are generally known as heteroreceptors. In the hippocampus, activation of excitatory inputs can trigger APs in GABAergic interneurons causing a widespread increase in extracellular GABA levels. Specifically, short-lasting repetitive stimulation in the CA1 region of the hippocampal slice determines heterosynaptic depression of excitatory synaptic transmission mediated by presynaptic $GABA_B$ metabotropic receptors (Isaacson et al., 1993).

Feedback mechanisms have been identified involving several retrograde messengers released postsynaptically to influence release from the presynaptic terminal. They can signal through G-protein coupled receptors located on presynaptic terminals to modulate synaptic communication. There are many neuromodulators such as dopamine, dynorphin, glutamate and oxytocin, released in response to synaptic activity following the liberation of vesicles in the extracellular space, that affect the postsynaptic targets usually exerting an inhibitory effect over transmission (Drake et al., 1994; Feigenspan

et al., 1998; Kombian et al., 1997). Retrograde messengers are also released by non-vesicular mechanisms. At hippocampal synapses, endocannabinoids are released from the postsynaptic cell following the cleavage of lipid precursors. This release of endocannabinoids leads to an inhibition of neurotransmitter release that lasts for tens of seconds (Wilson, Nicoll, 2002). In the cerebellum, retrograde signaling suppresses both excitatory and inhibitory synapses (Kreitzer, Regehr, 2001). Active molecules such as anandimide and 2-AG (2-Arachidonoylglycerol) are produced by cleavage of phospholipids and are sensed by CB1 receptors on presynaptic terminals to regulate the release of neurotransmitter.

1.3 Functional role of STP and effects on network dynamics

Several different functional roles have been proposed for synaptic dynamics. STP can modulate the way presynaptic neurons act on their postsynaptic targets. In general, a synapse dominated by STF, allows information transfer for high-frequency bursts, which increase the synaptic strength. Conversely, a synapse with depressing behavior favors information transfer for low firing rates, since high-frequency spikes rapidly deactivate the synapse. One function of synaptic depression is to mediate sensory adaptation, which allows strong responses to novel stimulation and diminished responses to repeated stimuli (Chung et al. 2002). Short-term depression provides a mechanism for gain control, by assigning high gain to slowly firing afferents and low gain to rapidly firing afferents (Abbott, 1997) in order to produce equal postsynaptic responses to variable input frequencies. It has also been proposed that STP contributes to working memory (Deng, Klyachko, 2011). Working memory can be defined as a buffer to store for short periods information required to carry out complex cognitive tasks such as learning. Computational analyses have shown that such working memory operations can be mediated by calcium-dependent synaptic facilitation in the recurrent connections of neocortical networks. In a model proposed by (Fortune, Rose, 2001), short-term depression and facilitation operate at discrete synapses and frequency-dependent facilitation following synaptic depression might occur at a single synapse. Neurons in the CNS usually receive many synaptic contacts and the convergence of depressing and facilitating afferent synapses would lead to the generation of a temporal filtering function. Temporal filtering properties arise from the interplay of particular

combinations of short-term synaptic depression and facilitation in response to afferent stimulation (Fig. 1.5).

Synaptic plasticity has been usually evaluated measuring the responses to periodic stimulation frequencies or pairs of pulses from a resting state, and those patterns seem to be insufficient to elicit the emergent temporal processing typical of complex biological sensory systems. Studies (Abbott, Regehr, 2004; Buonomano, Maass, 2009) have confirmed that short-term plasticity might also contribute to temporal processing and the employment of biologically relevant temporal patterns of afferent stimulation appears fundamental to unravel the mechanisms of plasticity. Classic slice experiments carried out in the hippocampus showed that natural stimulus patterns are capable of adjusting synaptic strength. In particular it was suggested (Dobrunz, Stevens, 1999) that synaptic strength is very strongly modulated during natural synapse use by STP using natural action potential trains recorded *in vivo* from awake animals as stimulus patterns for synaptic recordings *in vitro*. In another study, responses of excitatory and inhibitory hippocampal synapses to natural spike trains were evaluated (Klyachko, Stevens, 2007). Spike trains were recorded from place-cell firing in freely moving rodents and used as stimulation patterns. The authors found that under this stimulation with physiological patterns, excitatory and inhibitory synapses act as adaptive filters with STP properties that allow them to selectively change the connections' strength during epochs of high-frequency discharge at near-physiological temperatures. In both types of synapses, synaptic strength is characterized by an almost constant level during low activity and another near-constant, but elevated (for excitatory synapses) or reduced (for inhibitory synapses) level during high-frequency epochs.

A number of functional roles for STP have been specified here but the list is far from complete. What seems clear is that short-term synaptic plasticity can drastically alter how a neuron activates its postsynaptic targets and that patterns of activation and details of spike timing have a profound influence on synaptic strength. The next paragraph will present how synaptic dynamics can be modulated in a system that is strategically relevant in our project: the somatosensory TC pathway.

1.4 Information dynamics in the TC pathway

As already mentioned, in the visual, auditory and somatosensory systems, information is transmitted to higher processing areas through TC synapses. In the rodent brain, TC synapses mediate specific inputs from four different parallel pathways dedicated to the transmission of whisker-related sensory information to the somatosensory cortex. The principal driver pathway from TC to the barrels represents the main input to the cortex with glutamatergic neurons in the VPM thalamic nucleus sending information relating primarily to deflections of a single whisker. The axons of VPM neurons converge in individual layer 4 barrels contacting both inhibitory and excitatory neurons. TC connections have been classically described as strongly depressing in several *in vitro* (Gil et al., 1997, 1999; Stratford et al., 1996) and *in vivo* (Chung et al., 2002; Bruno, Sakmann, 2006) experiments (Fig. 1.6A,B). The common element of these studies consists in evaluating the depressing effect on TC connections of a periodic stimulation starting from rest. The sensory stimuli used to unravel the TC integration in the barrel cortex *in vivo* have usually been stereotypical whisker deflections, thanks to their technical simplicity. But in natural conditions sensory stimuli usually consist of irregular pattern of temporal events.

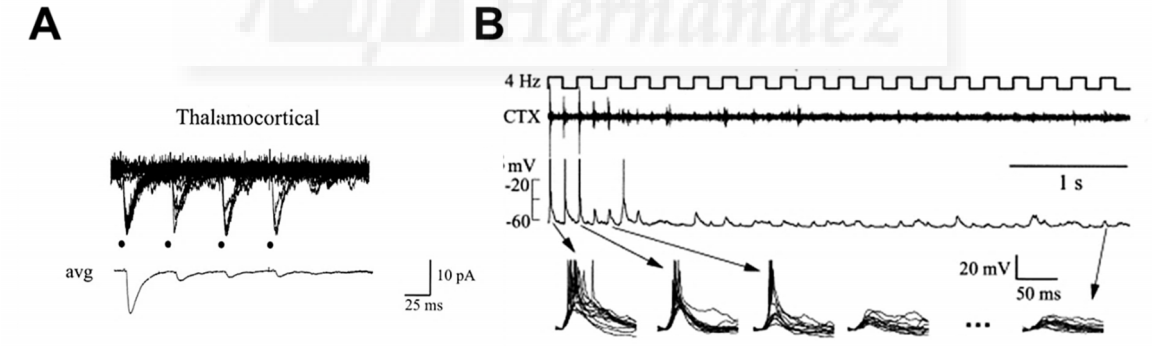

Figure 1.6: Short-Term Dynamics of TC connections.
A, *In vitro* all-or-none EPSCs evoked from a TC connection in mice slices. Top: ten consecutive responses to a train of four stimuli at 20 Hz. Bottom displays the average traces. Dots represent stimulation times. Modified from (Gil et al., 1999) **B**, Top: simultaneous extracellular multiunit recordings from barrel cortex (CTX) during 4 Hz stimulation of the primary whisker (B1) in anaesthetized rats. Bottom: intracellular responses of a cortical neuron in the C1 barrel to a 4 Hz stimulation of the primary whisker. Upper trace is a single trial. Multiple repetitions (n = 12) of the first four and the last onset responses in the train are shown below at expanded time scale. Modified from (Chung et al., 2002).

Recently it has been shown that responses of neurons in the barrel cortex can be notably different when obtained with regular or irregular whisker stimulation patterns (Lak et al., 2008; Lak et al., 2010). Moreover in natural conditions external stimuli arrive to the cortex alongside a complex and rich background of spontaneous and evoked activity. Indeed, a big effort has been made in living animals to demonstrate a possible repercussion of the brain state on information transmission in the neural network. This work has shown that short-term dynamics at TC synapses are dependent on the level of prior activity (Reig et al., 2006; Castro-Alamancos, 2004; Castro-Alamancos, Oldford, 2002; Boudreau, Ferster, 2005), and the impact on information processing can be very profound. For instance, STD in cortical slices is reduced as a function of the spontaneous ongoing activity in the network (Reig et al., 2006): depression is strongly diminished in ferret slices displaying spontaneous rhythmic slow oscillations in comparison with silent slices. Other evidence (Castro-Alamancos, 2004) shows that short-term depression in the neocortex is affected by the behavioral state: *in vivo*, sensory adaptation mainly occurs during quiescence because sensory-evoked responses are strong, while during behaviorally activated states, sensory responses are weaker and adaptation is less present. This weakening of sensory response, or sensory suppression, may be caused by activity-dependent depression of TC synapses. Globally, these effects could lead to fewer but more synchronized cells responding to a specific stimulus. In this way TC synapses could focus the response only to salient sensory stimuli in order to produce a clear network outcome giving rise to a specific behavior.

Although there is a tendency for STP to be remarkably different *in vitro* than *in vivo*, with many studies showing stronger STD *in vitro* than *in vivo*, this may be an effect of multiple differences in experimental conditions between *in vivo* and *in vitro*. These include the diverse ionic environment in living animals compared to slice protocols (Reig et al., 2006), the animal age, given that synapses from younger animals usually employed for *in vitro* recordings have stronger STD (Reyes and Sakmann, 1999), and the presence of neuromodulators *in vivo* (Gil et al., 1997). As already said, heterogeneous behavior is seen depending on the type of stimulation as well as on the brain state or behavioral activity. Analyzing the effects of realistic stimulation on STP could be important to our understanding of the mechanisms governing plasticity of neural networks during information processing.

1.5 Diverse TC short-term plasticity elicited by ongoing stimulation

A previous study by our group (Diaz-Quesada, Martini et al., 2014) showed that STP is variable across TC synapses. As demonstrated in earlier work (Gil et al., 1999; Gabernet et al., 2005) TC connections stimulated from rest (silence) using a pattern of regular intervals display depression to steady state (Fig. 1.7A). In our work, based on measuring whole-cell responses of layer 4 neurons to stimulation of TC fibers, we found that synaptic dynamic behavior was surprisingly diverse across TC connections, when recorded during ongoing stimulation. A shift from regular (constant interval) stimulation to an irregular pattern consisting of different interstimulus intervals (ISIs) with identical average frequency (4.59 Hz) unveiled synaptic responses that could be dominated either by facilitation or depression (Fig. 1.7B): each connection responded in a distinct manner to irregular stimulation started from steady state (Fig. 1.7C). Having observed this striking variability among the STP within the lemniscal population of TC synapses, we wished to understand the ordering principles for this behavior.

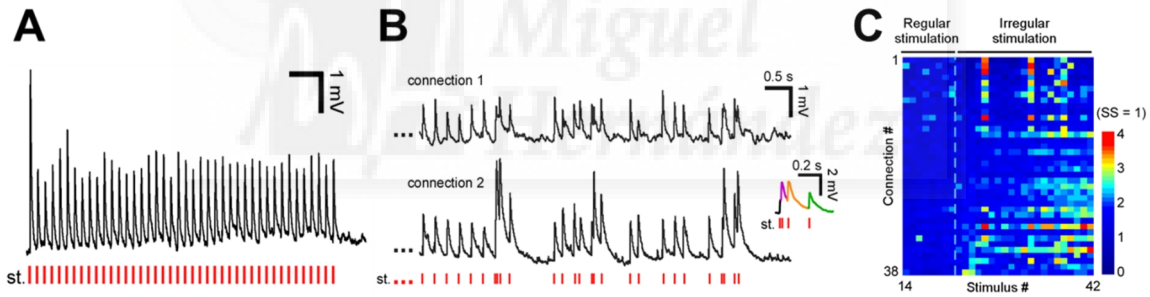

Figure 1.7: Diverse TC short-term plasticity elicited during ongoing stimulation.
A, Example TC connection depresses under regular stimulation from rest. The stimulus train (st.) is shown at the bottom in red. **B**, Diverse behavior of two example connections after a switch from steady-state regular stimulation to an irregular train with identical average frequency (stimulation pattern shown at bottom). Inset shows magnified PSPs of connection 2 immediately after switch; different colors correspond to successive PSPs. Both synapses depressed following stimulation from rest. Modified from (Díaz-Quesada, Martini et al., 2014). **C**, Diverse plasticity of PSP peaks across different connections. Stimulation was with a 42-pulse regular–irregular sequence as in **B**; plot begins at stimulus 14 in the sequence, while transition to the irregular train occurs at stimulus 22 (dashed line). Each row represents one connection (n = 38). For each connection, PSP peak magnitude is normalized to its value at steady state (left side of plot: s.s. = 1). Recordings (rows) are ordered from the smallest (top) to the largest (bottom) relative facilitation after the switch from regular to irregular stimulation.

2. Aims

In this project, we aimed to analyze the principles governing heterogeneous STP of excitatory TC connections under naturalistic, ongoing sensory inputs. We focused first on the underlying synaptic mechanisms and second on the possibility of cellularly regulated specificity, trying to address the following questions:

1. Mechanisms

- ✓ Do inhibitory pathways contribute to the diversity of STP of TC evoked responses?
- ✓ Is the observed STP diversity caused principally by pre or post-synaptic factors?
- ✓ Do specific modulators of transmitter release play a regulatory role in setting the level of STP across synapses in the population?

2. Specificity

- ✓ Are differences in plasticity regulated at cell level?
- ✓ Are postsynaptic layer 4 neurons sensitive as a whole for particular stimulus frequencies?

3. Materials and methods

All procedures complied with national and European Union policies for the care and use of animals in research. The experimental approach chosen for this work consisted of performing electrophysiological intracellular recordings from neurons in a reduced preparation: TC acute slices taken from mice (Agmon, Connors, 1991). This is a classical approach used by many groups over the years to characterize synaptic dynamics. We chose it because it gave us the possibility to vary experimental parameters for synaptic stimulation in a highly controlled manner. TC slices were obtained from ICR mice between 13-25 postnatal days of age of either sex. At this stage in development, the critical period for TC synaptic plasticity is closed (Crair, Malenka, 1995) and the period when sensory responses have been described as facilitating has ended (Borgdorff et al., 2007).

3.1 Intracellular whole cell recordings

Most of the experiments performed in this project use the patch-clamp whole cell recording technique (Sakmann, Neher, 1984). These recordings allow measuring the voltage or current across the membrane of a cell. To make an intracellular recording, the tip of a sharp microelectrode, usually a glass capillary, must be brought into contact with the cytoplasm. The glass micropipettes are filled with a solution that has a similar ionic composition to the intracellular fluid. A chlorided silver wire inserted into the pipette connects the electrolyte to the amplifier and signal processing circuit. The voltage measured by the electrode is compared to the voltage of a reference electrode, usually a silver chloride-coated silver wire in contact with the extracellular fluid around the cell. To achieve the start of the recording, the patch pipette mounted on a headstage is moved towards the cell through brain tissue using a micromanipulator. Positive pressure controlled with a manometer is applied before reaching the cell in order to avoid small debris to block the cell's tip. The potential difference between the pipette and the reference electrode is then zeroed before touching the surface of the cell. After that, positive pressure is diminished while the pipette is gently moved towards the target cell until its surface is touched and the pipette resistance increases, reaching values in

the range of one GigaOhm. Gentle suction is applied through the microelectrode to draw a piece of the cell membrane (the "patch") into the microelectrode tip; the glass tip forms a high resistance "seal" with the cell membrane. This configuration is called "cell-attached" mode, and it can be used for studying the activity of the ion channels that are present in the patch of membrane. If more suction is now applied, the small patch of membrane in the electrode tip can be displaced, leaving the electrode sealed to the rest of the cell. This "whole-cell" mode allows very stable intracellular recording.

3.1.1 Current clamp recordings

Most of our experiments were performed using the current clamp technique. The current clamp technique records the membrane potential by injecting current into a cell through the recording electrode. Unlike in the voltage clamp mode, where the membrane potential is held at a level determined by the experimenter, in "current clamp" mode the membrane potential is free to vary, and the amplifier records whatever voltage the cell generates on its own or as a result of stimulation.

3.1.2 Voltage clamp recordings

In the voltage clamp technique it is possible to "clamp" the cell potential at a given value thanks to an electronic feedback circuit: in particular the difference signal between the voltage command and the membrane voltage is used by the voltage clamp amplifier to generate a current that is injected via the recording electrode to the target cell. This near-simultaneous circuit feedback keeps the membrane voltage and the command voltage as close as possible.

3.2 Recording conditions

Patch clamp recording experiments were carried out in a conventional set-up that consists of: a vibration isolation table, a recording chamber, a microscope coupled with

an infrared camera and TV monitor, a headstage, two micromanipulators, an amplifier, a computer and an analog-to-digital board (Fig. 3.1).

A vibration isolation table (TMC63-531) was needed to minimize undesired mechanical movements that could affect recordings. The recording chamber, connected to the perfusion system, was the place where slices were positioned one by one, resting on the bottom of the chamber and submerged in Artificial Cerebro-Spinal Fluid (ACSF). ACSF was constantly bubbled with carbogen (95%O_2, 5% CO_2) and flowing from the perfusion system into the chamber and constantly changed thanks to a vacuum system in order to have always a fresh ACSF. In some experiments a heating coil was used connected to the perfusion system to perform recordings at controlled temperature. An Olympus BX51w1 microscope connected to an infrared camera (Till Photonics VX55) sending the image to a TV monitor was used to visualize the slices.

Slices were visualized with a 4x objective (Olympus) to choose the area of interest.

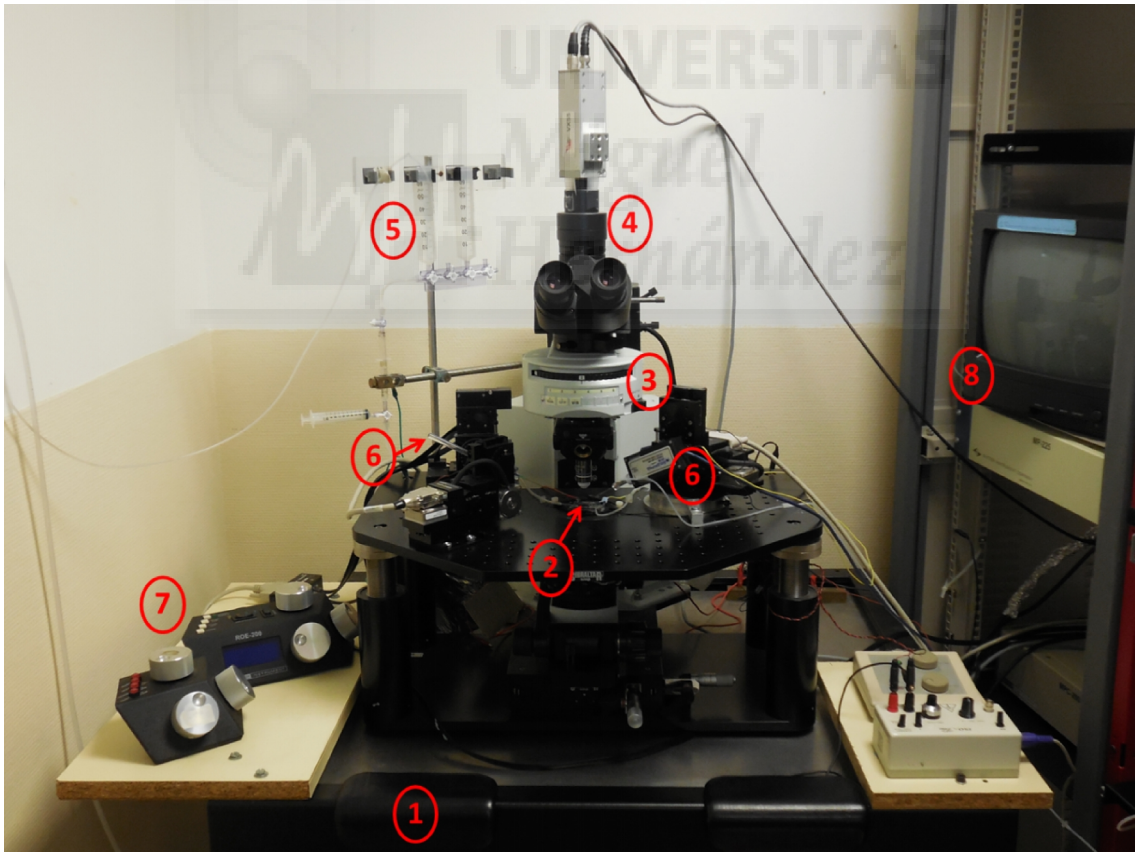

Figure 3.1: Experimental setup.
Picture of the experimental setup used for most of the experiments carried out. 1) vibration isolation table. 2) recording chamber. 3) microscope. 4) infrared camera. 5) perfusion system. 6) headstage and pipette holder. 7) micromanipulators. 8) TV monitor.

Barrels were clearly visible as dense rounded spots under 4x magnification in TC slices (Figs. 3.2A, 3.4A). To select excitatory neurons in layer 4 we used differential interference contrast microscopy (DIC) under 40x magnification (Olympus). Thanks to this technique, contrast in transparent and unstained samples is enhanced to give the appearance of a three dimensional object. Neurons were then selected based on morphological criteria. Cells with small spherical cell bodies (~10–15 μm in diameter) and dendrites confined to L4, typical of spiny stellate neurons, were chosen (Fig. 3.2C,D). Glass pipettes pulled so that their tips achieved an appropriate shape (width and taper) and resistance (3-6 MΩ) (Narishige PC-10) were mounted to the headstage and used to record the cells of interest. The headstage was a preamplifier connected to the main amplifier (Axon Multiclamp 700-B, Molecular Devices, Union City, CA). Pipettes were moved using a micromanipulator (Sutter MP-285) that allows to accurately control the movement in the three different directions (x,y,z) within submicron range. The main amplifier (Axon Multiclamp 700-B) was connected to a computer and an analog-to-digital board (PCI 6040-E, National Instruments).

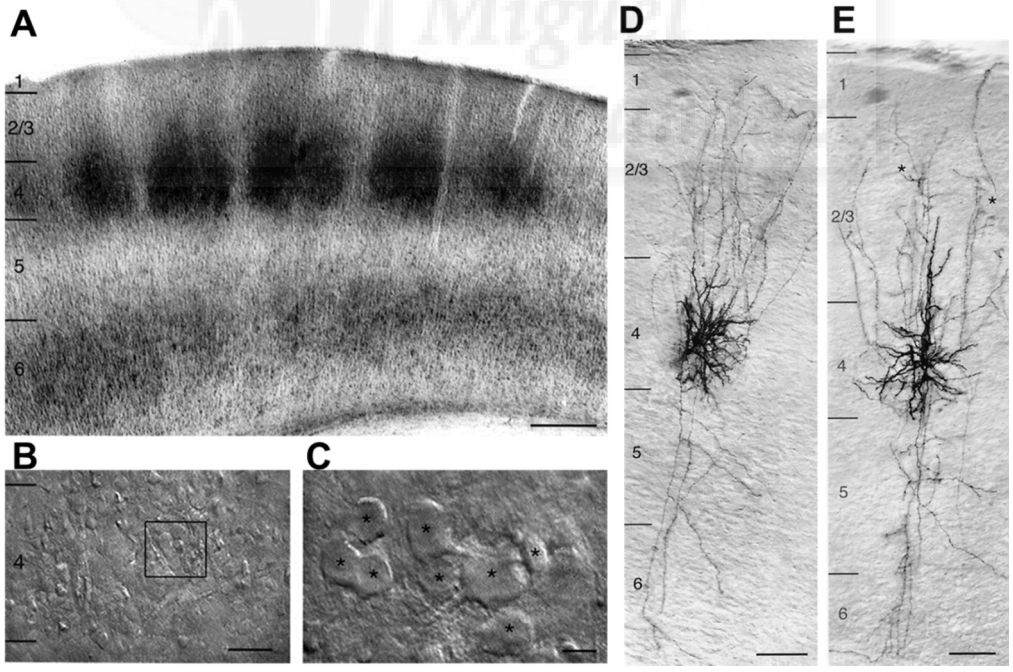

Figure 3.2: Barrel structure in the somatosensory cortex.
A, Low magnification of a semicoronal section through the barrel field stained for cytochrome oxidase showing the regular distribution of barrels in layer 4. Scale bar, 500 μm. **B**, Low magnification IR-DIC contrast image of layer 4 of the barrel cortex. Scale bar, 200 μm. The black box indicates a cluster of spiny layer 4 neurons marked by black asterisks shown enlarged in **C**. Scale bar, 10 μm. **D**, Micrograph of the synaptically coupled pair of spiny stellate cells

labeled with biocytin in comparison with a synptically coupled pair of star pyramidal cells (**E**). Scale bar, 100 μm. Modified from (Lubke et al., 2000).

3.2.1 Whole cell recordings

Patch electrodes were pulled from borosilicate glass (1.5 mm outer diameter, 0.86 mm inner diameter; Harvard Apparatus and WPI) and filled with internal solution containing (in mM) 130 K-methylsulfonate, 10 Na-phosphocreatine, 10 HEPES, 4 $MgCl_2$, 4 Na_2-ATP, 3 Na-ascorbate, and 0.4 Na_2-GTP (unless otherwise specified); pH 7.33, 287-303 mOsm. Alexa 594 (Invitrogen) or DNDS 1 mM (Tocris) were added to the internal solution in subsets of experiments. Recordings were mainly performed at room temperature (24ºC), with some at 32-34ºC.

Recordings were not corrected for liquid junction potential. Neurons were classified according to their response to depolarizing square pulses of 500 ms duration and increasing intensity ranging from 50 pA to 400 pA with 50 pA steps. Only neurons with the regular spiking (RS) phenotype (McCormick et al., 1985), clearly distinguishable from fast spiking (FS) cells or low threshold spiking cells (LTS), the other two main categories found in the layer 4 (see Introduction, Fig. 1.4), were included in the analyzed data set. Input resistance was in the range 150-500 MΩ and access resistance was under 10% of input resistance; recordings were discarded if access resistance was unstable or the resting membrane potential drifted by more than 10 mV. Data were acquired, filtered at 4-10 kHz, and sampled at 20 kHz under the control of software custom-written in Matlab (The Mathworks) (Pologruto et al., 2003).

3.2.2 Slice preparation

Slices (350 μm thickness) were prepared following conventional methods (Diaz-Quesada, Maravall, 2008). Briefly, after sacrificing the animal, the brain was removed and placed in ice-cold cutting solution bubbled with carbogen (95% O_2, 5% CO_2) and containing (in mM): 110 Cl-choline, 25 $NaHCO_3$, 25 D-glucose, 11.6 Na-aspartate, 7 $MgSO_4$, 3.1 Na-pyruvate, 2.5 KCl, 1.25 NaH_2PO_4, 0.5 $CaCl_2$. The brain was split at the midline and each hemisphere glued to a custom-made aluminium wedge at a slope of

50º. On the surface of the wedge 2 lines making an angle of 10º were visible to help placing the two hemispheres. Specifically the left hemisphere was glued onto the right part of the aluminium wedge-shaped piece lying on the internal side with the frontal lobe facing down while the right hemisphere was glued to the other side (Fig. 3.3A). Slices were cut on a vibratome (Integraslice 7550M; Campden Instruments) (Fig. 3.3B) and transferred to a chamber containing ACSF continuously perfused with carbogen. The first slices were discarded until the hippocampus, thalamus and fornix were clearly visible (Agmon and Connors, 1991; Land and Kandler, 2002).

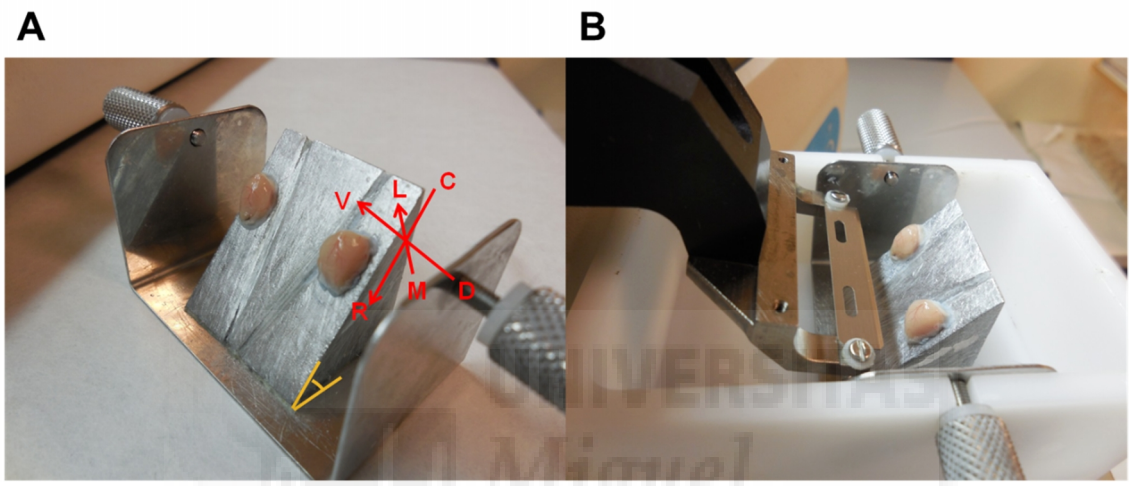

Figure 3.3: Cutting procedure of TC slices with the vibratome.
A, The right hemisphere (right part of the wedge in the picture) is glued on the left part of the wedge lying on its medial face while the left hemisphere is glued on the right part of the wedge lying on its medial face. Rostral part of the hemispheres is directed towards the bottom of the cutting chamber, caudal part (without the cerebellum) is just opposite to the rostral direction. The dorsal part of both hemispheres is located distal to the two diagonal lines on the surface of the wedge. The angle in orange defines a 50º slope. R: rostral; C: caudal; M: medial; L: lateral; V: ventral; D: dorsal. **B**, Wedge with glued hemispheres placed in the cutting chamber for slicing procedure.

An average of 3 slices per hemisphere were collected for each experiment and then incubated in ACSF at 34°C for ~30 minutes prior to recording and then kept at room temperature until used. Low-calcium concentration (low-[Ca^{2+}]) solution ACSF contained in mM: 127 NaCl, 25 $NaHCO_3$, 25 D-glucose, 2.5 KCl, 1.25 NaH_2PO_4, 2 $MgCl_2$, 1 $CaCl_2$. This gave a [Ca^{2+}] closer to physiological values than conventional ACSFs for in vitro recording. High calcium concentration (high-[Ca^{2+}]) solutions ACSF contained in mM: 127 NaCl, 25 $NaHCO_3$, 25 D-glucose, 2.5 KCl, 1.25 NaH_2PO_4 and 1 $MgCl_2$, 2 $CaCl_2$ for 2 mM extracellular calcium solution; 0,5 $MgCl_2$, 4 $CaCl_2$ for 4 mM extracellular calcium solution.

3.2.3 Solutions and drugs

Most of the recordings were made at room temperature except for a few experiments where a higher temperature (34ºC) was used. The majority of the experiments were performed using a standard low-[Ca^{2+}] while other experiments were done with high-[Ca^{2+}].

For NMDA blocking experiments we added to the standard ACSF the NMDA antagonist RS-(CPP) ((*RS*)-3-(2-Carboxypiperazin-4-yl)-propyl-1-phosphonic acid) or the NMDA antagonist D-APV (D-(-)-2-Amino-5-phosphonopentanoic acid), both from Tocris Bioscience, Bristol, UK.

For voltage clamp experiments a modified internal solution was used containing (in mM): 135 $CsMeSO_4$, 8 NaCl, 10 Hepes, 0.5 EGTA, 4 Mg-ATP, 0.3 Na-GTP, 5 Qx-314. For inhibition blockade experiments DNDS was added to the usual internal solution (see Materials and Methods 3.2.2).

For kainate receptor manipulation we used a number of different antagonists against multimeric receptors: UBP296 ((*RS*)-1-(2-Amino-2-carboxyethyl) -3- (2-carboxybenzyl)pyrimidine-2,4-dione), UBP310 ((*S*)-1-(2-Amino-2-carboxyethyl) -3-(2-carboxy-thiophene-3-yl-methyl) -5- methyl-pyrimidine-2,4-dione) and UBP316 (ACET) ((S)-1-(2-Amino-2-carboxyethyl) -3- (2-carboxy-5-phenylthiophene-3-yl-methyl) -5- methylpyrimidine-2,4-dione), all from Tocris Bioscience, Bristol, UK, and NS-102 (6,7,8,9-Tetrahydro-5-nitro-1H-benz[g]indole-2,3-dione 3-oxime) from Sigma-Aldrich Seelze, Germany. Additionally we performed current clamp experiments on TC slices using knock-out (KO) mice for the GluK1 (Mulle et al., 2000) and double KO for GluK1 and GluK2 (Mulle et al., 1998) subunits, obtained by crossing the GluK1 and GluK2 mouse lines (courtesy of Juan Lerma laboratory, Instituto de Neurociencias, San Juan de Alicante).

Adenosine receptor manipulation was made using the subtype A1 receptor (A1R) agonist adenosine (9-β-D-Ribofuranosyladenine, Adenine riboside, Adenine-9-β-D-ribofuranoside, Tocris Bioscience, Bristol, UK**)** and two different antagonists, DPCPX (8-Cyclopentyl-1,3-dipropylxanthine, Tocris Bioscience, Bristol, UK) and 8-CPT (8-Cyclopentyl-1,3-dimethylxanthine, Sigma Aldrich, Seelze, Germany).

3.3 Stimulation

An external Pt-Ir concentric bipolar electrode (FHC; outer pole diameter 200 µm, inner pole diameter 25 µm) connected to a stimulus isolator (Iso Flex; A.M.P.I.) was placed in the white matter (Fig. 3.4A). Stimulation amplitude was determined based on the minimal stimulation approach (Raastad et al., 1992; Stratford et al., 1996; Gil et al., 1997; Gil et al., 1999), as follows. We applied single depolarizing square current pulses of 0.1 ms duration; amplitude was gradually increased until a clear PSP was seen in a fraction of trials. Slightly lowering stimulus amplitude led to complete response failure; slightly increasing amplitude caused an increase in response reliability with no observed change in latency, magnitude or shape (Fig. 3.4B).

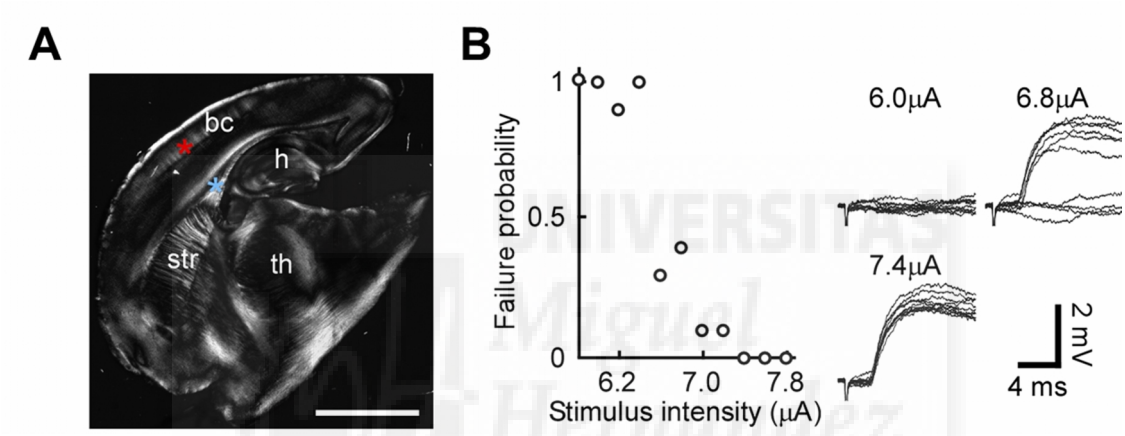

Figure 3.4: Recording configuration and stimulation parameters.
A, TC slice configuration. bc, Barrel cortex; th, thalamus; h, hippocampus; str, striatum. Asterisks indicate typical sites for recording (red) and stimulation (blue). Scale bar, 1 mm. **B,** Protocol for setting stimulus amplitude. There was a clear distinction between failed and successful trials (with PSPs evoked at fixed latency). Stimulus amplitude was set at the minimum level that gave no stimulation failures. Modified from (Díaz-Quesada, Martini et al., 2014).

We set the final magnitude at the latter level, such that response failures to temporally isolated single stimuli were not observed over ~10 repetitions. This approach ensured that failures of stimulation were negligible while the number of stimulated fibers was kept low (putatively as low as 1). Stimulus amplitudes were 1-15 µA, towards the lower end of previously reported thresholds for TC activation and an order of magnitude lower than thresholds for antidromic activation of corticothalamic neurons (Rose, Metherate, 2001). After setting the stimulus amplitude as above, we checked that repetitive stimulation continued to produce successful responses with unchanging latency and

stereotypical shape throughout the train of stimuli. Response characteristics remained stable over the course of the experiment; otherwise, the recording was discarded.

In a subset of experiments we used a more powerful stimulation protocol in order to verify the possibility of a post-synaptic clustering of STP properties. The logic was to attempt to increase the number of stimulated fibers to measure whether a larger number of different synapses onto a neuron behaved similarly to synapses taken individually. Taking as reference the stimulation magnitude defined as above, we doubled it to set the final magnitude.

In the standard synaptic stimulation protocol, a sequence of four different stimulation patterns was presented for several times (usually ten each) during the recording session. Each of the different stimulation patterns consisted of 42 pulses for a 9 second-long train and was obtained as a combination of regular and irregular trains having the same mean frequency of 4.59 Hz but different inter-stimulus intervals (Fig. 3.5). Here, we use "irregular" simply to denote a sequence with variable intervals and an aperiodic arrangement. The irregular train was extracted from a recording of whisker-evoked action potential activity in the VPM thalamic nucleus of a urethane-anesthetized rat (Petersen et al., 2008).

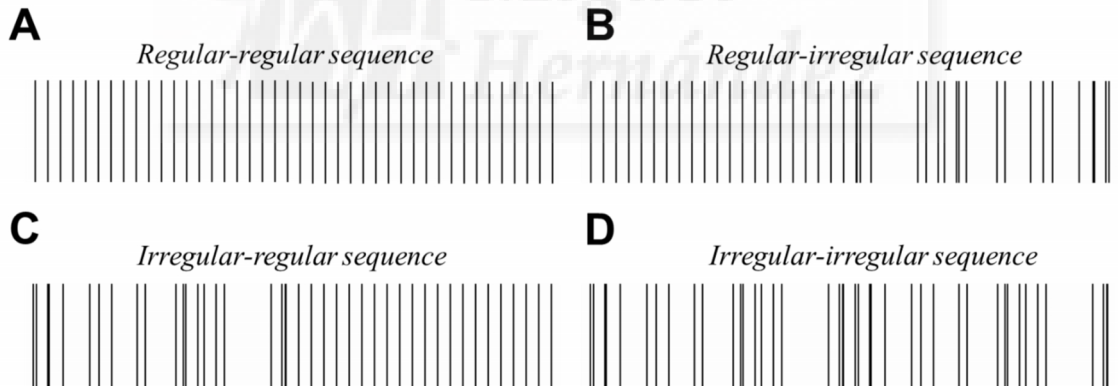

Figure 3.5: Pattern of stimulus sequences.
Schematic representation of the four different stimulus sequences used in our recordings: **A**, R*egular-regular* sequence; **B**, *Regular-irregular* sequence; **C**, *Irregular-regular* sequence; **D**, *Irregular-irregular* sequence.

It therefore consisted of activity that TC synapses might experience in the live animal. It is important to note, however, that the specific pattern of stimulation was not critical, because earlier experiments from our group found that during ongoing stimulation, STP behavior is governed principally by the single most recent ISI (Diaz-Quesada, Martini et al., 2014; see section 3.7). As a consequence of this, characterizing STP did not require

a larger set of stimulus protocols, e.g. reproducing the exact sequences of presynaptic activation that each connection undergoes *in vivo*. The four patterns contained respectively two regular trains (*regular-regular* stimulation), a regular train followed by a switch to the irregular one (*regular-irregular*), an irregular followed by a regular train (*irregular-regular*), and two consecutive irregular trains *irregular-irregular*). All stimuli were generated in Matlab.

3.3.1 White noise stimuli

In a series of experiments we used noise currents injected through the recording electrode into the soma of the neurons while stimulating the white matter with a bipolar electrode as previously described (Materials and Methods 3.2). We added this type of stimulus in order to make the recorded neuron more susceptible to fire action potentials. The stimuli were generated by creating a vector of stochastic numbers derived from a Gaussian distribution, giving rise to a normally distributed white-noise stochastic waveform. The vector was then filtered with a Gaussian waveform in the time domain, with a standard deviation of 2 ms, obtaining a filtered noise time series whose values fluctuated on a timescale of a few milliseconds. In this set of experiments we used ten different noise stimuli, each of which had a mean value centered at 0 pA, therefore we referred to them as "symmetric noise" stimuli. In all the experiments, 4 different synaptic stimulation patterns were used while recording from layer 4 excitatory cells: a regular train followed by another regular train (*regular-regular*), an irregular one (*regular-irregular*), a shuffled irregular train (same intervals but randomly switched in order; *regular-shuffled*) and a Poisson distributed interval train (*regular-poisson*). This was done to ensure that a broad range of ISI values was well sampled and in order to allow detection of pattern preferences present in neurons (any preferences of individual synapses were, in general, predicted at the single ISI timescale, as described in section 3.7, but this was unknown for neurons a priori). Each synaptic stimulation pattern was repeated 10 times, with a different noise waveform injected into the neuron on every trial. Because the intracellularly injected waveform was different from trial to trial, any systematic response observed across trials was caused by the synaptic stimulation pattern.

3.4 Pharmacological manipulation

3.4.1 Inhibitory blockade

STP diversity might be caused by differences in the rate of depression of the disynaptic inhibitory component of PSPs relative to the monosynaptic excitatory component. To evaluate this possibility, we conducted a set of experiments with the intracellular $GABA_A$ antagonist dinitrostilbene-2,2'-disulfonic acid (DNDS), a chloride channel blocker, added to the patch pipette (Dudek, Friedlander 1996; Covic, Sherman, 2011). To verify the effect of DNDS, we carried out separate voltage-clamp experiments and measured the reversal potential of evoked TC synaptic currents 12 ms after the stimulus, the empirically determined time of maximal conductance (Fig. 3.6). In these experiments, TC EPSCs reversed at the glutamatergic reversal potential (0 mV) rather than at the hyperpolarized potential found in the absence of DNDS (n = 3) (Fig. 4.3A, Results). DNDS concentration was 0.5 mM (n = 16) or 1 mM (n = 9): no effect of varying the concentration was observed (p = 0.485, 2-dimensional Kolmogorov-Smirnov test), so experiments with different concentrations were pooled together.

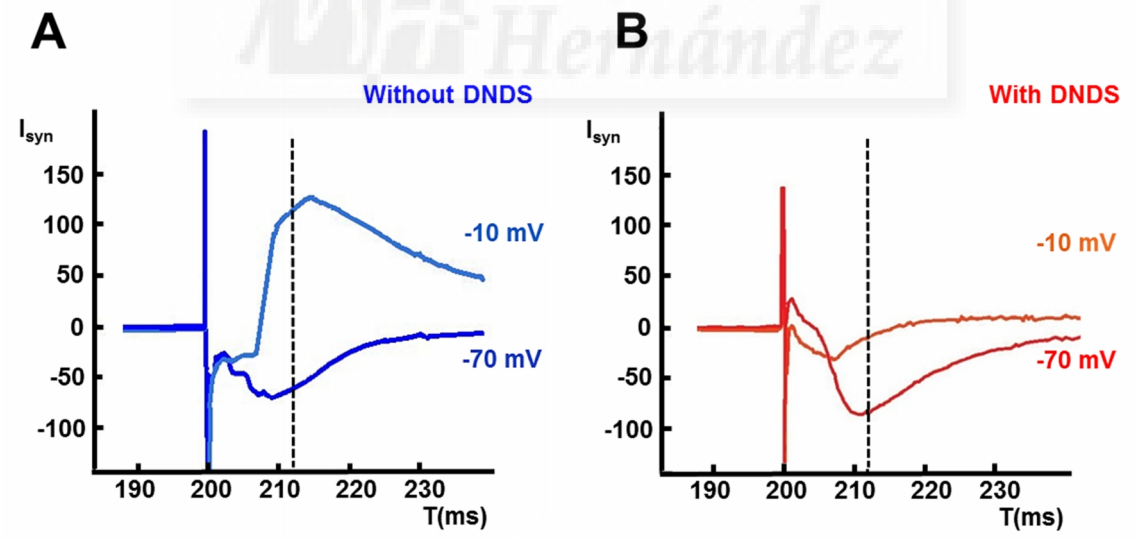

Figure 3.6: Verification of DNDS-mediated block of inhibition.
Voltage clamp recordings at two different Vm (-70 mV and -10 mV) showing currents in the absence (**A**) (dark blue and light blue traces) and presence (**B**) (red and orange traces) of DNDS. At -70 mV in both conditions (dark blue and red) the currents evoked are similar; without DNDS at -10 mV there is a clear inhibiting current (light blue trace) that disappears in the recordings made using DNDS (orange trace). Plots display the average of 5 repetitions for each condition.

3.4.2 Adenosine receptor modulation

It has been shown that adenosine receptors can play a role in modulating synaptic transmission. To check for a possible involvement of adenosine receptors in STP diversity we performed whole cell current clamp recordings using the A1R agonist adenosine (100μM) and two different antagonists, 1μM DPCPX and 1 μM 8-CPT in the bath.

3.4.3 Kainate receptor modulation

To check for a role of kainate receptors in explaining the diverse STP we used different drugs that block a specific subunit of the receptor, the GluK1: 10 μM UBP296, 10 μM UBP310, 200 nM UBP316 (ACET), and 20 μM NS-102 in the recording bath.

3.5 Fluorescent probe (AAV1/9.hSynapsin.iGluSnFR) injections to visualize glutamate neurotransmission

3.5.1 In utero injections

Injections were carried out in collaboration with Lopez-Bendito laboratory, Instituto de Neurociencias, San Juan de Alicante. AAV1.hSynapsin.iGluSnFR or AAV9.hSynapsin.iGluSnFR injections were performed to infect thalamic VB neurons reaching layer 4 in the cortex or cortical cells. The glutamate sensor iGluSnFR carried in the construct is a reporter able to signal excitatory release from neuronal terminals (Marvin et al., 2013). Pregnant females at different stages (E11.5 and E13.5) were deeply anesthetized with isofluorane to perform laparotomies and the embryos were visualized through the uterus with a fiber-optic light source. The constructs, AAV1.hSynapsin.iGluSnFR or AAV9.hSynapsin.iGluSnFR at various dilutions were injected into the third ventricle in E11 for thalamic injections or in the cortex at E13.5 for cortical injections and mixed with 1% fast green (vol/vol, Sigma). Each embryo was injected through a glass capillary with a Vevo VisualSonics injector (Toronto, Ontario,

Canada). The surgical incision was then closed and embryos were allowed to develop until they reached P13. From this stage it was possible to begin to prepare TC slices for imaging and recording experiments as previously described.

3.5.2 Two photon setup

TC slices were placed into the same set-up as described in section (3.2.2). After choosing the barrels of interest, TC fibers were stimulated with a Pt-Ir concentric bipolar electrode positioned in the white matter, laterally to the selected barrel, as described in section 3.3. Barrels were visualized using a DM6000CFS microscope (Leica Microsystems) equipped with a water immersion lens (HCX IRAPO L 25x, numerical aperture 0.95, water immersion objective, Leica Microsystems). A two-photon laser scanning system (upright Leica DMFLSA stage) was used to image neuronal processes. Ultrafast pulsed laser beam (Spectra Physics Mai Tai HP) was set to 910 nm wavelength for imaging iGluSnFR. Images were captured using line mode scanning (512x512 pixels, 400 Hz; bidirectional (= 800Hz, lines/second) and acquired with the acquisition software LAS AF with Electrophysiology module, Leica Microsystems. Light was collected with external NDD (nondescanned photomultiplier detectors), with light filtered as follows: FITC/TRITC barrierfilter 1 BP585/40 (565-605nm), barrierfilter 2 BP525/50 (500-550nm).

3.6 Statistical analysis

All statistical analyses were performed with Matlab. We used different statistical tests depending on the distribution of the data. For each comparison, the test used is reported together with the results.

3.7 Data analysis

Mean PSP amplitude was computed for each stimulus in a train after removing stimulus artifacts by median filtering. To compute PSP amplitude, we searched for the

first membrane potential peak in the window extending from 0.5 ms to 12 ms after the stimulation pulse and subtracted a baseline averaged over 2 ms immediately preceding the stimulation pulse (Fig. 3.7). This short baseline effectively compensated for depolarization caused by earlier PSPs.

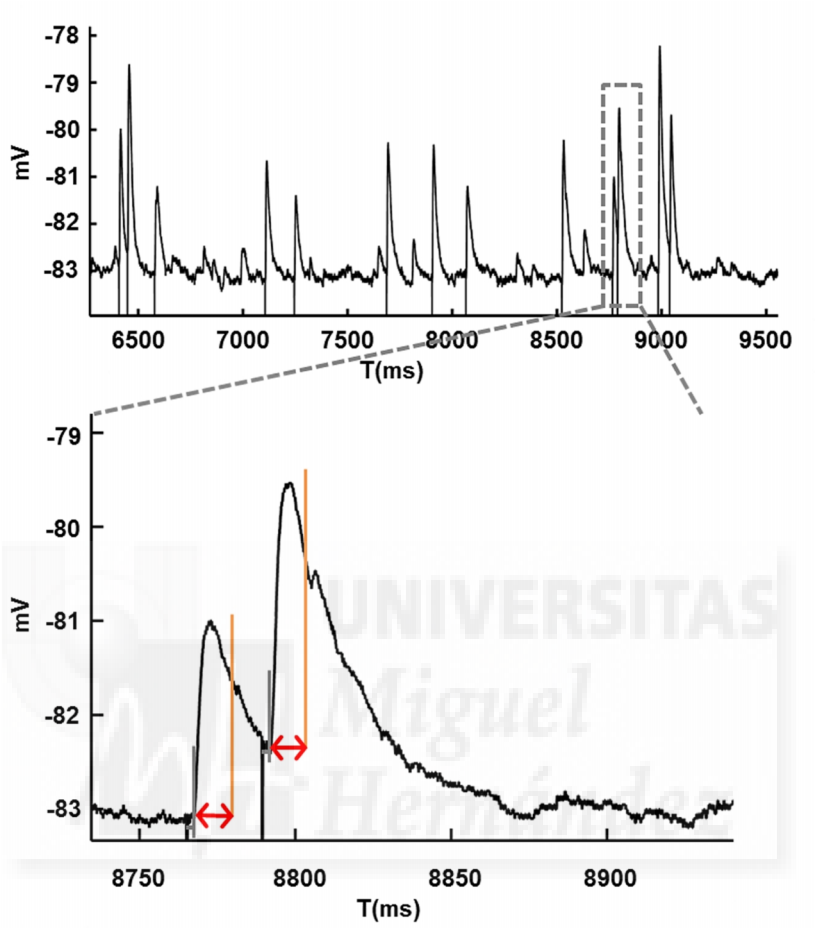

Fig. 3.7: Mean PSP amplitude computation.
Plot showing the postsynaptic response to the last 3000 ms of a *regular-irregular* train of stimulation (**Top**). For transparency, stimulation artifacts have been kept. (**Bottom**) inset showing the PSPs evoked by two pulses separated by a short ISI. Maximum membrane potential was sought within the window extending from 0.5 ms (grey line) to 12 ms (orange line) after the stimulation pulse. Membrane potential was averaged over 5 points (from -.1 ms to .1 ms relative to the raw peak), and a baseline averaged over 2 ms immediately preceding the stimulation pulse subtracted. Note the separation of time scales: the fast rise time relative to the slow EPSP decay and to the ISI, and the short baseline averaging window, permit baseline compensation in estimating EPSP peak amplitude.

To compute the **steady-state response level**, we considered PSPs evoked during regular stimulation (starting with the first train, *regular-regular* or *regular-irregular* stimuli). We discarded the first five PSPs (i.e., approximately the first second of stimulation) and computed mean steady-state PSP amplitude by averaging over all remaining PSPs evoked during regular stimulation. Steady-state depression was evaluated by taking the

ratio of the steady-state PSP amplitude to the average PSP amplitude in response to the first pulse in the train (also sometimes referred to as the "adaptation ratio" in the literature). Ratios < 1 indicated depression.

We computed a **facilitation index** to measure the relative response upon switching from regular to irregular trains during ongoing stimulation, as follows. First, we averaged the PSP amplitudes evoked by the second and third pulses after the switch to irregular stimulation, to reduce the dependence on a single, specific interval value. Then, we obtained the facilitation index as the ratio of this quantity to the steady-state PSP amplitude just before the switch. This parameter is a straightforward measurement of relative changes in response upon switching from constant-rate stimulation to a high instantaneous rate. The facilitation index was averaged for each connection by stimulating with the same pattern at least ten times per recording; each trial lasted 10 s, including periods of silence during which baseline properties were monitored.

Tuning curves for each synaptic connection were computed by plotting PSP magnitude as a function of ISI. After constructing the tuning curve for irregular stimulation, a tuning curve slope (TCS) (Fig. 3.8A,B) was fit by linear regression to the initial part of the tuning curve (including only small interval values, shorter than the regular interval, 218 ms), or to the late part of the curve (large intervals, longer than regular), or to the full curve. All three possibilities produced a significant negative correlation between the resulting TCS and the facilitation index described in the previous paragraph (Fig. 3.8C; see explanation below), but the fits based on the initial part of the tuning curve gave the tightest empirical correlation. Hence, we present results for the initial (fastest timescale, < 218 ms) part of the curve. Connections with smaller responses to short intervals (i.e., to high instantaneous frequencies) had positive TCS (Fig. 3.8A), while connections with larger responses to short intervals negative TCS (Fig. 3.8B). To characterize STP on a synapse-by-synapse basis, for each connection TCS was plotted against the facilitation index (Fig. 3.8C). TCS provided a simple measure of whether a connection tended to respond more to shorter or to longer ISIs (Fig 3.8A,B), while the facilitation index quantified changes in the connection's response when switching the stimulus pattern from regular to irregular. The facilitation index was < 1 when the mean response amplitude was reduced after the switch and > 1 when amplitude was increased. In earlier work from the lab, we found that, empirically, variations in facilitation index across connections were well predicted by TCS (tight negative correlation; see Fig. 3.8C).

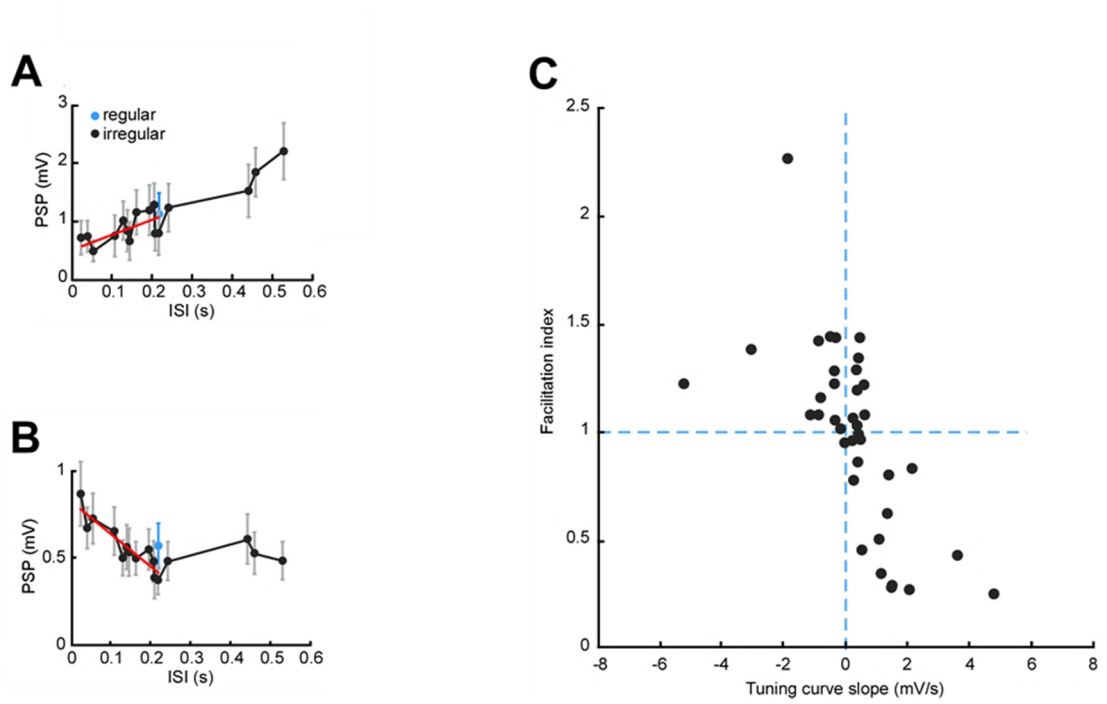

Figure 3.8: Population analysis of STP diversity.
A, Tuning curve showing dependence of PSP magnitude on ISI for a connection whose responses are smaller for short ISIs. Black, Responses to irregular stimulus; blue (single data point), responses to regular stimulus; red, linear fit to initial (short-interval) part of tuning curve. Error bars indicate SEM. **B**, Tuning curve for a connection whose responses are larger for short ISIs. Note the similarity of black and blue values in A and B, indicating tuning unaffected by whether the interval is within a regular or irregular train. **C**, Facilitation index (relative response after switch from regular to irregular stimulation) plotted against TCS across the population. Index is normalized such that 1 = no increase compared with steady state. Modified from (Díaz-Quesada, Martini et al., 2014).

This implied that TCS generated using a single arbitrary temporal pattern of stimulation, or even a set of stimulus trains at different constant frequencies, should predict responses for any other arbitrary pattern of ongoing stimulation. This notion was confirmed empirically (Diaz-Quesada, Martini et al., 2014).

4. Results

4.1 Regulation of STP heterogeneity

In our laboratory it has been recently shown in the rodent somatosensory whisker system (Diaz-Quesada, Martini et al., 2014), that ongoing, naturalistic stimulation alters the observed STP. Specifically, rather than being uniformly depressing, STP becomes strikingly diverse across TC connections. This diversity takes the form of variable tuning to the latest interstimulus interval: some connections respond weakly to shorter intervals, while other connections facilitate (Materials and methods, Fig. 3.8). We aimed to find ordering principles for this heterogeneity in STP across TC connections. Plasticity can be variable from one synapse to another even in apparently homogenous populations connecting neurons of a given class. Different synapses commonly exhibit different forms of STP. Diversity can be observed even across synapses of one neuron onto multiple target cells (Markram et al., 1998). It is possible that STP is specifically regulated at the pre- or postsynaptic cell level.

To understand the principles governing STP and describe its potential effects on sensory encoding in the TC pathway, we focused on two main factors: the mechanisms underlying STP heterogeneity and the possible rules for specificity across synapses connecting to a single specific neuron.

4.2 Mechanisms underlying STP heterogeneity

We wondered which mechanisms contribute to determining diverse STP across TC synapses. We examined first whether it is a monosynaptic or disynaptic form of plasticity, evaluating the contribution of inhibitory pathways. Second, we tried to understand if STP diversity can be attributed to presynaptic mechanisms by evaluating the effects of varying extracellular calcium concentration and of NMDA receptor antagonists. Finally, we examined how diverse STP is regulated by specific modulators of transmitter release, taking into account two families of receptors, adenosine receptors and kainate receptors.

4.2.1 Contribution of inhibition to STP heterogeneity

First we considered the contributions of excitatory and inhibitory components to the postsynaptic potentials evoked by TC stimulation. The diversity we found across connections could potentially be explained by the contribution of a feedforward mechanism involving inhibitory neurons. In addition to the excitatory monosynaptic pathway connecting ventrobasal (VB) thalamic projection neurons to layer 4 of somatosensory cortex, there is a disynaptic pathway formed by collateral axons of VB projecting neurons that reach inhibitory neurons in layer 4, which project in turn to thalamorecipient cells in layer 4 (Fig. 4.1). During stimulation, this disynaptic inhibition could modify the balance between excitatory and inhibitory currents received by the thalamorecipient cell, giving rise to different responses (Gabernet et al., 2005; Wilent, Contreras, 2005). It is possible that a phenomenon observed as facilitation of the monosynaptic excitatory response in layer 4 neurons, could in fact be depression of the disynaptic inhibitory component, leading to an effective increase in the magnitude of the PSP. Depression of the TC drive to inhibitory cells could even potentially cause a failure in firing of interneurons, inducing the disynaptic response component to fall out altogether.

4.2.1.1 STP heterogeneity has a monosynaptic locus

To rule out the possibility that STP diversity could be explained by a variable contribution of inhibition we performed a set of experiments adding the intracellular $GABA_A$ antagonist DNDS, a chloride channel blocker, to the intracellular solution contained inside the patch pipette (Dudek, Friedlander 1996; Covic, Sherman, 2011) (see Materials and Methods, 3.4.1). DNDS inhibits $GABA_A$-ergic inhibitory post-synaptic potentials; it diffuses in the post-synaptic cell from the recording electrode restricting the inhibition blockade to the patched cell. DNDS avoids the need to add other non-selective $GABA_A$ antagonists to the bath such as Gabazine, that would lead to hyperexcitability of the slices. To check that DNDS is effective in layer 4 neurons under our experimental conditions, we determined in voltage-clamp experiments the reversal potential of evoked TC synaptic currents measured 12 ms after the stimulus (Materials and Methods, Fig. 3.6) with the membrane holding potential clamped at steps from -90 mV to 0 mV. In these experiments, TC EPSCs reversed at the glutamatergic reversal

potential (0 mV) rather than at the hyperpolarized potential found in the absence of DNDS (n = 3, Fig. 4.3A).

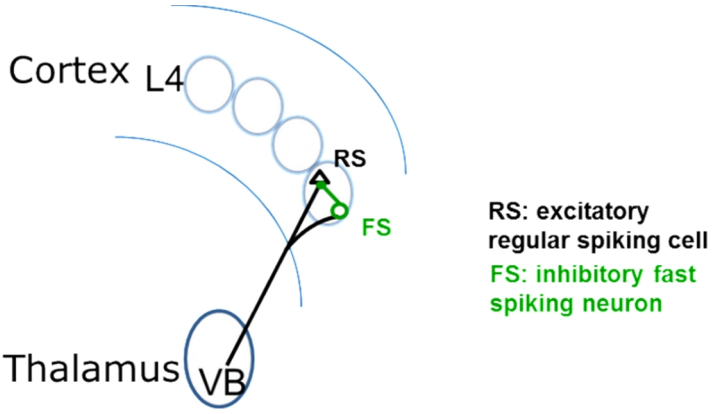

Figure 4.1: Disynaptic pathway to L4 of the somatosensory cortex.
Schematic drawing of the disynaptic pathway formed (1) by collateral axons of thalamic VB projecting neurons to inhibitory FS cells in layer 4; FS cells (2) subsequently contact RS excitatory neurons, thus determining a powerful disynaptic inhibition that shapes the net effect of thalamic activation upon the cortical target.

We performed current clamp experiments with DNDS in the intracellular solution (0.5 or 1 mM), recording from layer 4 excitatory neurons while stimulating TC fibers with two different patterns, the *regular-regular* train and the *regular-irregular* one (see Materials and Methods, 3.4.1). Recordings performed with 0.5 mM (n = 16) and 1 mM (n = 9) gave indistinguishable results (p = 0.49, 2-dimensional Kolmogorov–Smirnov test), so data were pooled together and compared with control experiments with intact inhibition (Fig. 4.2).

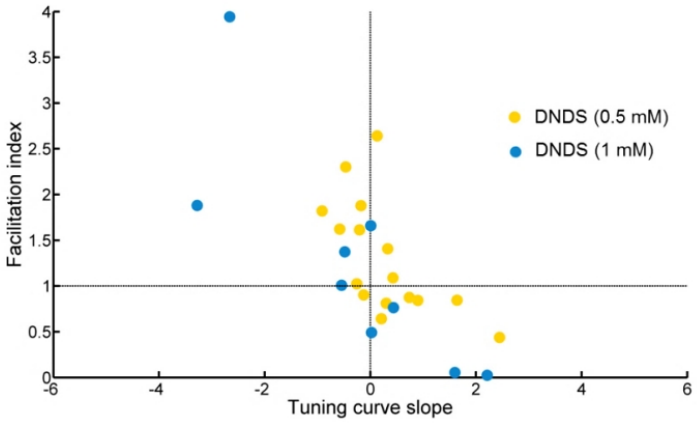

Figure 4.2: Effect of inhibitory blockade at different DNDS concentrations.
Facilitation index plotted against tuning curve slope of recordings made with 0.5 mM (n = 16, yellow dots) or 1 mM (n = 9, light blue dots) DNDS in the intracellular recording solution. No difference between the two distributions was observable.

Although DNDS eliminated the inhibitory contribution to synaptic responses (Fig. 4.3A), the distributions of facilitation index and TCS showed no significant changes in DNDS recordings compared to controls (Fig. 4.3B; p = 0.34, 2-dimensional Kolmogorov-Smirnov two-sample test; n = 25 for DNDS, n = 22 for controls).

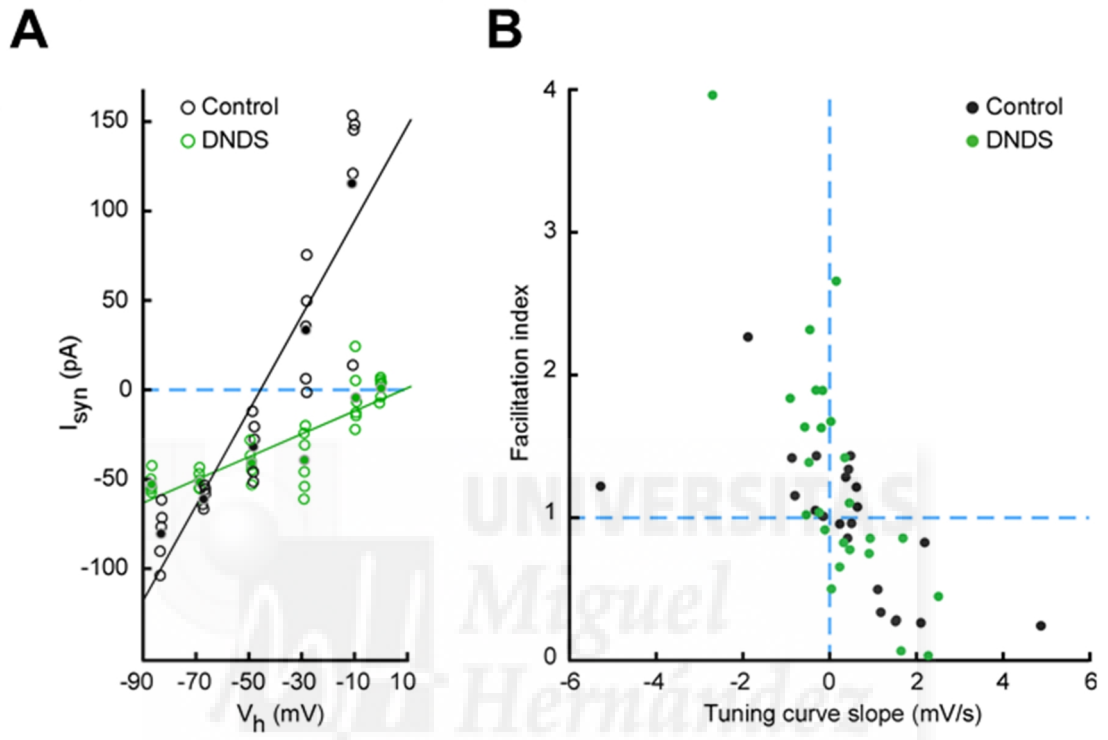

Figure 4.3: Effect of inhibitory blockade on STP diversity.
A, I–V curves constructed from EPSC responses in voltage-clamp from two different neurons in the same slice, without (black) and with (green) DNDS in the internal solution. The slight difference in holding potential (V_h) among points at each nominal holding potential is caused by correction for a voltage drop across the series resistance. Note absence of synaptic response at the reversal potential for excitation (around 0 mV) with DNDS. **B**, Facilitation index plotted against TCS for experiments with and without DNDS in the recording pipette (control, n = 22; DNDS, n = 25). Note the similarity between the two distributions. Modified from (Díaz-Quesada, Martini et al., 2014).

Therefore diversity in STP of TC synapses during ongoing stimulation does not require a variable contribution of disynaptic inhibition, but instead is determined by properties of monosynaptic excitatory connections.

4.2.1.2 Variability in excitation-inhibition dynamics

Although the presence of inhibition was not necessary for observing STP diversity, it was still possible that inhibitory pathways displayed variable STP just as excitatory connections did.

To evaluate excitatory-inhibitory dynamics we performed voltage clamp experiments using the same configuration as before, stimulating TC fibers with an extracellular electrode while recording from excitatory neurons in layer 4. A modified intracellular solution was used, containing $CsMeSO_4$ instead of potassium methanesulfonate and QX-314 to eliminate sodium currents. Cesium acts as a potassium (K^+) channel blocker so a cesium methanesulfonate intracellular solution blocks K^+ conductances.

Membrane potential was held at different values starting from hyperpolarized potentials to more depolarized (from -80 mV to 0 mV in steps of 20 mV) to calculate the amount of evoked current flowing through the cell. Excitatory and inhibitory post-synaptic currents (EPSCs and IPSCs) evoked by extracellular TC stimulation were calculated for each recording. Some connections were characterized by strong inhibiting currents after the switch from regular to irregular pattern of stimulation at more depolarized potentials (0, -20 mV) as shown in figure 4.4A, while others had very large EPSCs after the switch in the stimulus train (Fig. 4.4C). To calculate the balance between excitatory and inhibitory currents, the peak values (expressed in picoamperes) of the most hyperpolarized (-80 mV) and the most depolarized (0 mV) traces for each recording were divided and a ratio was obtained. Overall, of the 22 recordings, 15 (68%) exhibited a depolarizing/hyperpolarizing current ratio > 1 (Fig 4.4B), with relatively strong inhibition at transition while others (7 recordings, 32%) had a hyperpolarizing/depolarizing currents ratio < 1 with strong excitation at transition (Fig. 4.4D). This variability suggests that “facilitating” and “depressing” projections also have a different balance of excitation/inhibition dynamics.

In conclusion, the observed STP diversity of TC synapses during ongoing stimulation is caused by differences in the properties of monosynaptic excitatory connections, but synapses can also display additional differences in the dynamics of the disynaptic inhibitory component.

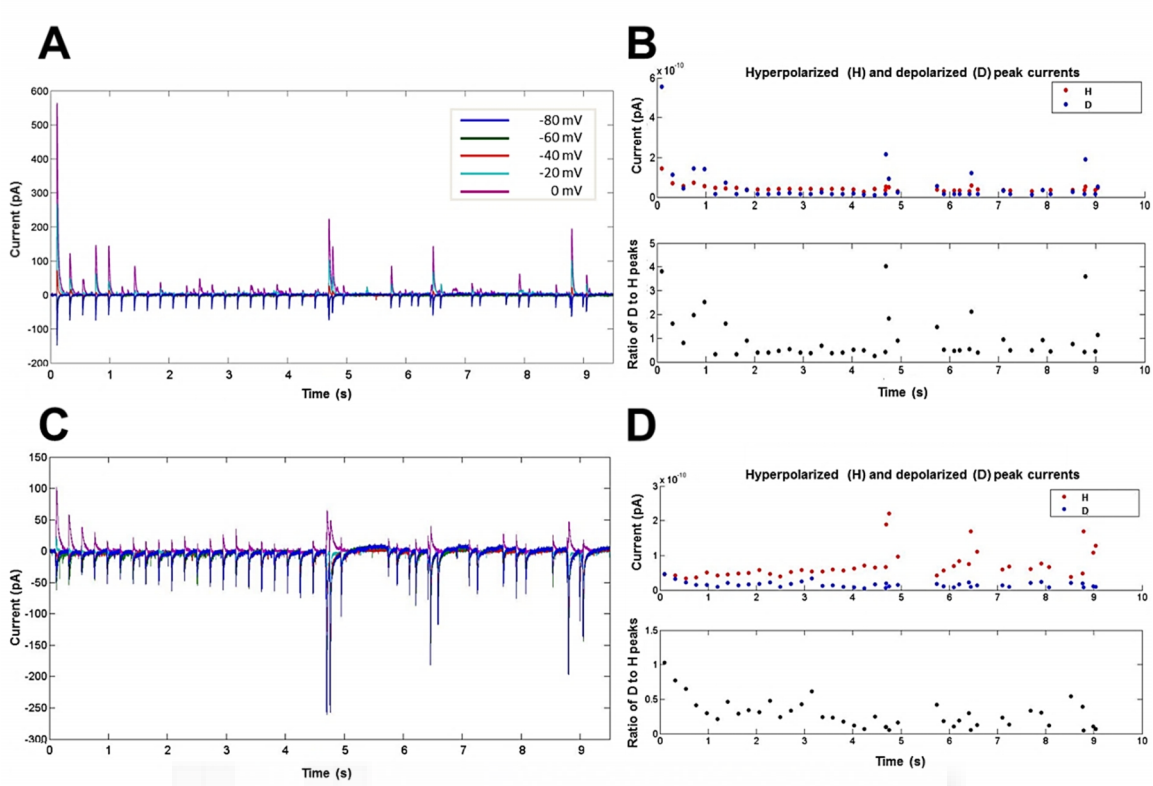

Figure 4.4: Excitatory and inhibitory currents balance.
A,**C**: Example traces of the response of two neurons to irregular stimulation at five different holding potentials (-80 mV, blue line; -60 mV, green line; -40 mV, red line; -20 mV, cyan; 0 mV, magenta line). Recording in **A** represents a cell in which the response after the switch in stimulation was characterized by strong inhibiting currents; recording in **C** represents a cell in which the response after the switch was characterized by strong excitatory currents. **B**: Top, peak currents expressed in picoamperes for the most hyperpolarized (-80 mV) and the most depolarized (0 mV) traces; bottom, ratio of depolarized to hyperpolarized current peaks is > 1 for cells behaving like in **A**. **D**: Top, peak currents expressed in picoamperes for the most hyperpolarized (-80 mV) and the most depolarized (0 mV) traces. Bottom, ratio of depolarized to hyperpolarized current peaks is < 1 for cells behaving like in **C**.

4.2.2 Is STP diversity a presynaptic mechanism?

Having demonstrated that STP diversity has a monosynaptic locus, we tried to determine whether the mechanisms underlying facilitation are principally pre- or post-synaptic, evaluating the influence of extracellular calcium concentration on neurotransmitter release and possible postsynaptic NMDA receptor-mediated effects on STP variability.

4.2.2.1 Calcium concentration has a significant influence on STP

An earlier data set (Diaz Quesada, Martini et al., 2014) included recordings at two different extracellular [Ca^{2+}] to evaluate if synaptic responses could be affected by changes in release probability and vesicle depletion, and at different temperatures (24ºC and 32-34ºC), a variable that has been shown to shift the response to irregular trains in the hippocampus (Klyachko, Stevens, 2006). One set of recordings was performed at a calcium concentration typical of slice experiments ([Ca^{2+}] = 2 mM), while the other one was closer to physiological values ([Ca^{2+}] = 1 mM) and was adopted for all the experiments described in the present dissertation. While STP was diverse for the considered groups (Fig. 4.5A), extracellular [Ca^{2+}] influenced STP (Fig. 4.5B), because there was significantly less depression at 1 mM than 2 mM (Diaz Quesada, Martini et al., 2014). Differently, temperature had no effect on STP heterogeneity, indicating little dependence of probability of release on temperature as shown in (Allen, Stevens, 1994). Thus [Ca^{2+}], but not temperature, has a significant influence on the distribution of STP values suggesting regulation by a presynaptic mechanism.

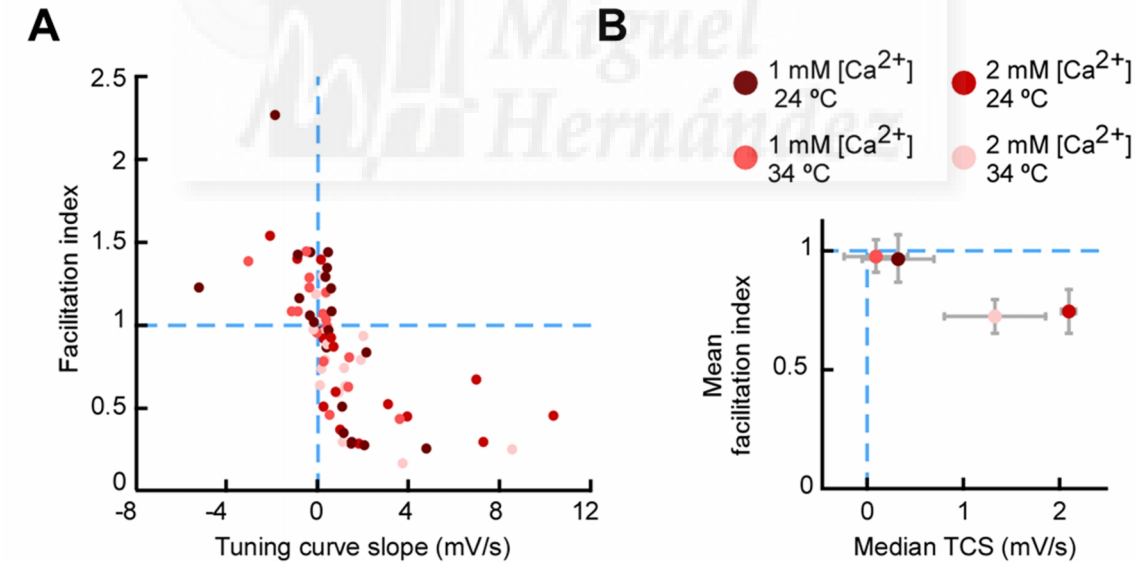

Figure 4.5: STP diversity across temperatures and extracellular [Ca $^{2+}$].
A, Facilitation index plotted against TCS for experiments conducted at different temperatures and extracellular [Ca $^{2+}$] values. Group sizes: n = 22 for [Ca $^{2+}$] 1 mM, temperature 24°C; n = 16 for [Ca $^{2+}$] 1 mM, temperature 32–34°C; n = 16 for [Ca $^{2+}$] 2 mM, temperature 24°C; n = 16 for [Ca $^{2+}$] 2 mM, temperature 32–34°C. Diversity occurred for all recording conditions. **B**, Central values across groups classified by recording condition. Consistent with a tendency toward depression, the mean facilitation index (post-switch response) was < 1, and the median TCS was positive (compare with dashed lines). Error bars indicate SEM. Modified from (Díaz-Quesada, Martini et al., 2014).

4.2.2.2 High calcium concentration affects STP variability

After showing that a higher [Ca^{2+}] determines an increase in release probability and consequently a greater depression, we wondered whether saturating the synaptic terminals with a high extracellular [Ca^{2+}] solution (4 mM) could have an effect on STP variability of the recording population.

To this end, we collected an additional data set of synaptic responses recorded under an extracellular calcium concentration (1 mM) close to the physiological values and after a fourfold increase in calcium concentration. The underlying idea is that an increase in [Ca^{2+}] leads to a more rapid depletion of presynaptic vesicles of the readily releasable pool, thus conceivably determining a change in the variability of STP. As expected, increasing the calcium to 4 mM induced initially higher EPSPs followed by faster depression; the distribution of the facilitation index changed significantly ($p = 0.015$, Wilcoxon signed-rank test, $n = 7$ recordings) showing a stronger depression than compared to 1 mM [Ca^{2+}] recordings (Fig. 4.6), although the TCS was not modified between different conditions ($p = 0.500$, Wilcoxon signed-rank test, $n = 7$ recordings).

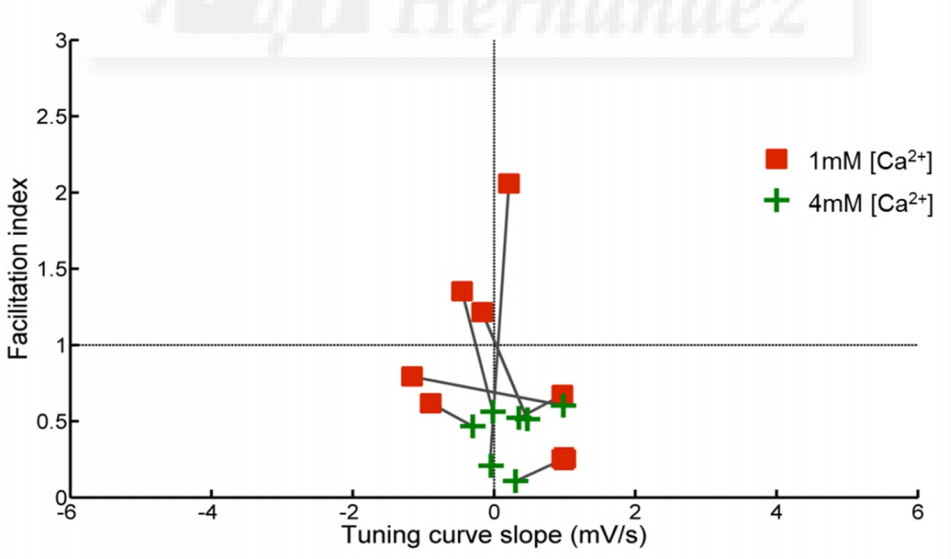

Figure 4.6: High calcium concentration effect on STP heterogeneity.
Plot showing the synaptic response of different connections ($n = 7$) under different extracellular [Ca^{2+}]. Elevating calcium concentration led to a decrease in facilitation index and a significant difference in STP distribution for the two recorded populations.

Moreover there was a significant reduction in STP heterogeneity ($p = 0.002$, 2-dimensional Kolmogorov-Smirnov two-sample test, $n = 7$ recordings). These results show that STP diversity is influenced by calcium concentration, supporting the possibility of a regulation by a presynaptic mechanism.

4.2.2.3 Effect of NMDA antagonists on STP

Excitatory glutamatergic synaptic transmission in the vertebrate brain is based on the release of L-glutamate from presynaptic terminals that diffuses across the synaptic cleft and binds to postsynaptic receptors. Activation of AMPARs is fast and transient, causing brief depolarizations that last no longer than a few milliseconds. NMDARs are not critical for this basal synaptic transmission, but instead they regulate functional and structural plasticity of individual synapses, dendrites, and neurons by allowing activation of specific calcium-dependent signaling cascades. Moreover, the NMDAR-mediated response is longer lasting and could potentially affect responses to later stimuli. To evaluate if heterogeneity in evoked synaptic responses was related to a specific activation of NMDA receptors we carried out experiments with either of two NMDA blockers (see Materials and Methods, 3.2.3). Either 10 μM of APV, a selective NMDA receptor antagonist that competitively inhibits the ligand (glutamate) binding site of NMDA receptors or 10 μM of (RS)-CPP, another potent and selective NMDA antagonist were added to the extracellular bath. We recorded layer 4 neurons in voltage clamp configuration while stimulating with a *regular-irregular* train of pulses. We recorded EPSCs at five different holding potentials (from -80 mV to 0 mV in 20 mV steps) and checked for possible effects of NMDA receptor blockade. Our data showed no significant differences in evoked currents after the shift from regular to irregular pattern in recordings with receptors blocked compared to controls. Taken together, the above experiments suggest that STP diversity depends on heterogeneity of presynaptic mechanisms.

4.2.3 Effects of neuromodulators on STP heterogeneity

Release properties of synapses in the central nervous system are highly variable, even across the same synaptic type. Heterogeneity in presynaptic function reflects differences in the intrinsic properties of the synaptic terminal and the activation of presynaptic neurotransmitter receptors. Activity dependent release can be influenced by differential presynaptic receptor activation. Having shown that diverse STP was not a consequence of a variable amount of inhibition but occurred across the population of monosynaptic excitatory TC connections, we focused on two presynaptic mechanisms that can regulate release probability and therefore plasticity. First we examined the role of adenosine receptors in modulating synaptic release. Then we assessed the effects of kainate receptors presynaptically expressed in TC synapses.

4.2.3.1 Effects of adenosine receptor modulation on STP diversity

One factor that can have a significant impact on synaptic release characteristics is susceptibility to modulation by local neurotransmitters, mediated by presynaptically expressed receptors (Zucker, Regehr, 2002). For example, adenosine has been shown to reduce synaptic excitation through the action of presynaptic receptors that inhibit the release of the excitatory neurotransmitter glutamate (Lupica et al., 1992; Shen, Johnson, 2003; Scanziani et al., 1992). Local action of extracellular adenosine at presynaptic A1 adenosine receptors (A1R) in hippocampal mossy fiber synapses maintains a low basal probability of transmitter release (Moore et al. 2003). Interestingly, application of adenosine decreases EPSCs elicited by stimulation of the VB thalamus in slice whole cell recordings (Fontanez, Porter, 2006). Therefore we sought to investigate whether release probability and STP in TC connections could be differentially modulated by adenosine receptors.

We conducted a first set of recordings using the same slice configuration as above while stimulating the white matter using two different stimuli, *regular-regular* and *regular-irregular* trains. We performed ten repetitions for each stimulus both under control conditions and after adding 100μM of adenosine to the bath. Adenosine addition clearly modified the release probability and STP of TC synapses. Specifically, applying adenosine increased the facilitation index ($p = 0.004$, Wilcoxon signed-rank test, $n = 11$

recordings), although TCS was not significantly modified (p = 0.965, Wilcoxon signed-rank test, n = 11 recordings). This dissociation of effects on facilitation index and TCS shows that the two quantities, although correlated, provide complementary information, and suggests that adenosine may have downregulated tonic release probability, enabling a larger relative increase in probability upon switches in frequency. The effect was to shift the distribution of STP values expressed by the population (Fig. 4.7). Of the four cloned adenosine receptors, A1, A2A, A2B, and A3, most of the inhibitory actions of adenosine on glutamate release have been ascribed to A1 receptors (Dunwiddie, Masino, 2001). For this reason we tried to evaluate the effect of the negative modulation of A1 receptors on STP, using the specific antagonists DPCPX and CPT.

We recorded evoked synaptic responses to TC stimulation in control conditions with normal ACSF in the bath and after addition of 1 μM DPCPX or 2 μM CPT (each in a separate set of experiments).

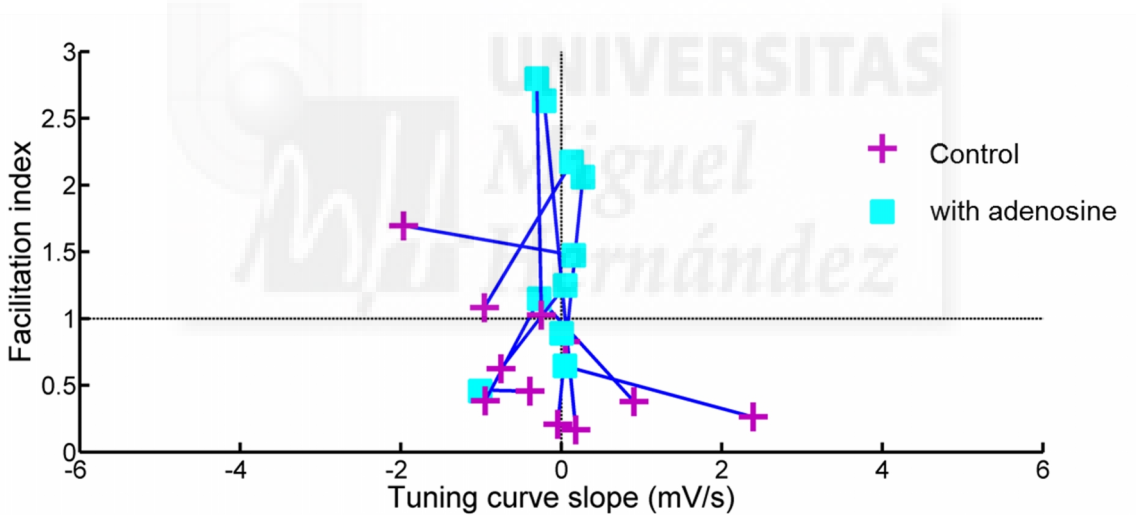

Figure 4.7: Adenosine effect on STP heterogeneity.
Plot showing the response of different connections (n = 11) in control conditions and after addition of adenosine to the recording bath. Adenosine addition led to an increase of the facilitation index although TCS is not significantly modified.

The inhibition of A1 receptors causes a significant change in TCS by making synapses relatively more responsive to long intervals (DPCPX: n = 12 recordings, p = 0.001, Wilcoxon signed-rank test; CPT: n = 6 recordings, p = 0.007, Wilcoxon signed-rank test). This can be interpreted as meaning that, because adenosine could not now limit release, there was a greater overall tendency towards depression, and release probability exhibited greater recovery after long intervals. Conversely, the difference in facilitation

index was not significant either for DPCPX or CPT recordings (DPCPX: n = 12 recordings, p = 0.605, Wilcoxon signed-rank test; CPT: n = 6 recordings, p = 0.078 Wilcoxon signed-rank test), again pointing to a dissociation between facilitation index and TCS. These effects again shifted the overall distribution of STP behaviors as compared to control (Fig. 4.8).

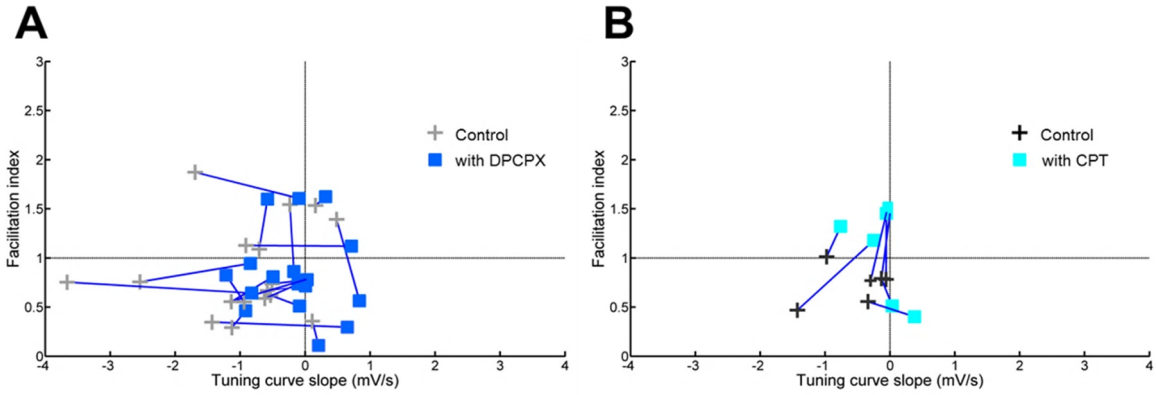

Figure 4.8: A1R antagonists effect on STP heterogeneity.
A, Plot showing the response of different connections (n = 12) in control conditions and after addition of DPCPX to the recording bath. **B**, Plot showing the response of different connections (n = 6) in control conditions and after addition of CPT to the recording bath. Both pharmacological manipulations led to the inhibition of A1 receptors causing a significant change in TCS by making synapses relatively more responsive to long intervals. No net significant difference in the facilitation index was seen.

In conclusion, the adenosine-receptor pathway modulated STP behavior of TC synapses. Specifically, applying adenosine enhanced facilitation while applying antagonists enhanced depression. However, altering the regulation of release by A1 receptors shifted behavior but did not eliminate diversity. That these pharmacological manipulations did not eliminate variability across synapses suggests intrinsic variability in the expression of the machinery for calcium entry and neurotransmitter release.

4.2.3.2 Effects of kainate receptors modulation on STP diversity

In the past few years, it has become clear that a major locus of kainate receptor expression and function is in, or near, the presynaptic terminal. Presynaptic kainate receptors are widely expressed in the mammalian brain and play an important role in synaptic transmission and STP. It has been shown in hippocampal preparations that activation of kainate receptors regulates glutamate release (Chittajallu et al, 1996) and

can both depress or facilitate transmission in different synapses at different stages of development. Presynaptic kainate receptors can up- or down-regulate both glutamatergic and GABAergic transmission in a dose-dependent manner (Kullmann, 2001; Lerma et al., 2001; Isaac et al., 2004) if stimulated with exogenous or endogenous ligands (Jiang et al., 2001; Kidd et al., 2002). Kainate receptors are structured as a tetramer formed by combinations of GluK1-5 subunits (Bettler and Mulle, 1995). GluK1-3, the low affinity kainate binding subunits, can form functional ion channels either as homomers or heteromers; on the contrary, GluK4 or 5 homomers (the high affinity kainate binding subunits) are not functional and are not surface expressed in neurons.

Kainate receptor function has been investigated and best described in the hippocampus. Bath application of the GluK1 antagonist LY382884 to neonatal hippocampal slices results in an increase in the presynaptic kainate receptor-mediated EPSC (Lauri et al., 2006). In neonates, the presynaptic kainate receptor displays a very high affinity and is activated by low levels of L-glutamate. This high affinity kainate receptor is lost during development together with the facilitation of synaptic responses in CA1 synapses.

Kainate receptors are widely expressed in primary sensory neocortex and can regulate TC inputs especially during development. In layer 4 of the neonatal BC, presynaptic kainate receptors at TC inputs can be activated by synaptically released glutamate during short bursts of high frequency trains to mediate a short-term depression (Kidd et al., 2002). During short bursts, synaptic transmission is depressed by up to about 60%. This effect is inhibited by the GluK1 antagonist LY382884, demonstrating an involvement of GluK1 containing receptors. Similarly to hippocampal kainate receptors, functional expression is developmentally regulated, with a clear decrease during the first postnatal week (Kidd, Isaac, 1999).

However, other aspects of how kainate receptors determine the regulation of TC transmission are still not well understood. For this reason we tried to modulate kainate receptor activity in order to evaluate putative effects on STP. We used multiple strategies to inhibit their action in juvenile animals (P14-P20), including both pharmacological blockade and KO mouse models for specific kainate receptor subunits. In separate experiments we recorded responses of layer 4 excitatory neurons to white matter stimulation after adding to the bath one of three different GluK1 subunit antagonists: 10 μM UBP 296 (n = 6), 10 μM UBP 310 (n = 10) and 200 nM UBP316 (ACET) (n = 3). Compared to the distribution of control experiments (n = 22), none of

the GluK1 antagonists provoked a clustering of the data or significant differences from controls (Fig. 4.9, p = 0.165 for UBP 296, p = 0.191 for UBP 310, p = 0.130 for UBP 316, 2-dimensional Kolmogorov-Smirnov two-sample test), implying that the inhibition of GluK1 subunit containing kainate receptors did not cause a shift in the population distribution of STP during ongoing stimulation. In another set of experiments we recorded responses to the same stimulus trains in slices obtained from KO mice for the GluK1 (n = 5) subunit or double KO for GluK1/K2 (n = 9). No differences were observable from control conditions (Fig. 4.9, p = 0.208 (GluK1), p = 0.758 (GluK1/K2), 2-dimensional Kolmogorov-Smirnov two-sample test) showing again no modulatory effect of KARs on TC synaptic STP. Since no effect on STP diversity was found in experiments conducted after having inhibited kainate receptors through the use of different antagonists, we performed additional "before and after" experiments, where the selective GluK1 antagonist UBP 310 (10 μM) was added to the bath after recording responses to TC stimulation in control conditions, to check if a difference could be appreciable within the recording session.

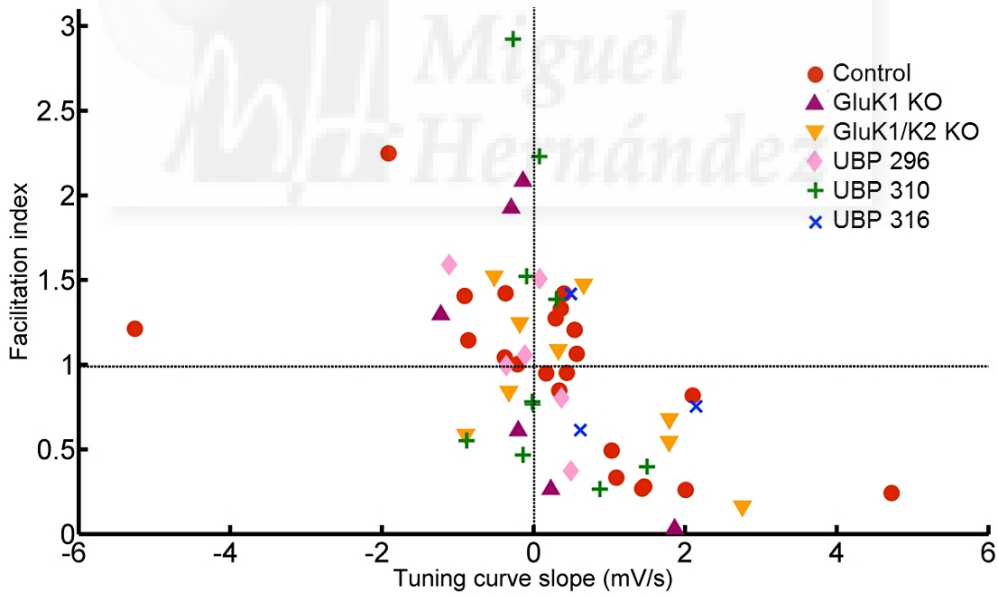

Figure 4.9: KAR manipulation effect on STP heterogeneity.
Facilitation index plotted against TCS comparing STP in control conditions (n = 22) or experiments performed using two different KO models (GluK1 KO, n = 5; GluK1/K2 KO, n = 9), and recording with the addition to the bath of UBP 296 (n = 6), UBP 310 (n = 10) and UBP 316 (n = 3). STP heterogeneity held for all the conditions tested.

This pharmacological manipulation did not have a consistent effect across the set of recordings, suggesting a lack of systematic modulation of STP by GluK1 receptors (Fig.

4.10, n = 9 recordings; p = 0.570, 2-dimensional Kolmogorov-Smirnov two-sample test ; p = 0.734 for TCS; p = 0.570 for facilitation index, Wilcoxon signed-rank test).

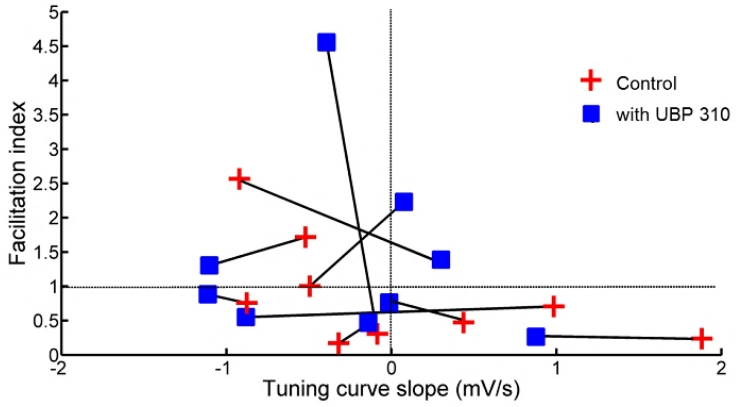

Figure 4.10: UBP 310 effect on STP heterogeneity.
Facilitation index plotted against TCS for experiments without (control n = 9) and after addition to the recording bath of UBP 310 (n = 9). There was no clear modulation of STP by GluK1 receptors.

In a further set of experiments aimed at determining kainate receptor modulation of STP, we used a different drug, NS-102, a selective kainate receptor antagonist that operates via the block of low-affinity $^{[3H]}$kainate binding to cortical membranes. NS-102 (20 μM) was added to the bath while EPSPs evoked in response to TC stimulation were recorded in current clamp whole cell mode configuration. Then facilitation index and TCS were compared between controls and after adding the antagonist (Fig. 4.11). No difference was found between the two conditions (p = 0.015, 2-dimensional Kolmogorov-Smirnov two-sample test; but p = 0.570 for facilitation index, Wilcoxon signed-rank test, n = 9 recordings; p = 0.054 for TCS, Wilcoxon signed-rank test, n = 9 recordings).

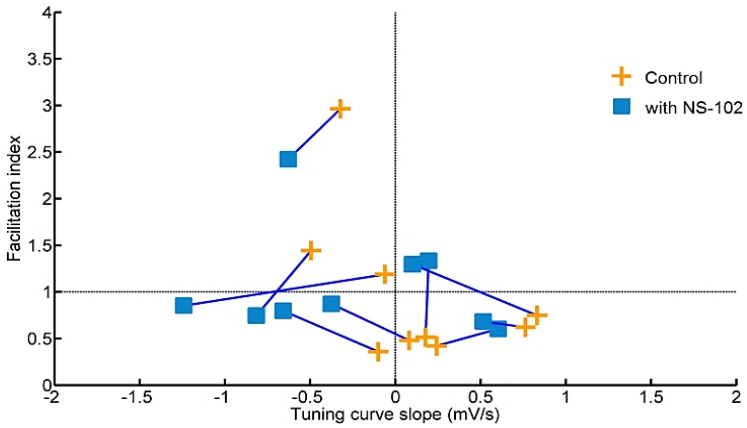

Figure 4.11: NS-102 effect on STP heterogeneity.

Facilitation index plotted against TCS for experiments without (control n = 9) and after addition of NS-102 (n = 9). There was no systematic shift of STP properties by using the blocker.

Considering the developmental downregulation of presynaptic TC kainate receptors described by some authors after the first postnatal week (Feldman et al., 1998; Kidd et al., 2002), the magnitude of their contribution to STP in juvenile or adult animals is unclear. We wondered whether the lack of systematic effect on STP during ongoing stimulation was due to a functional absence of kainate receptors, or whether the receptors were present but simply acted on STP at other epochs of stimulation – for example, in the initial phase of STP that occurs upon stimulation from rest. For this reason we analyzed a separate index of STP - the paired pulse facilitation (PPF) - in UBP 310 and NS-102 recordings. The result is that PPF was not higher compared to controls ($p = 0.083$ for UBP 310, $p = 0.275$ for NS-102, paired t-test) suggesting that presynaptic kainate receptors do not modulate early-phase STP in TC synapses at these ages.

4.3 Specificity underlying STP heterogeneity

A further key aspect of STP heterogeneity is whether differences in plasticity are regulated at cell level. If, for example, STP properties cluster presynaptically, all TC synapses projecting from a particular neuron will have similar dynamics. Conversely, STP could cluster postsynaptically (Yang, 2012), rendering each cortical neuron particularly sensitive to specific intervals. Both possibilities are not mutually exclusive. In this project we focused on postsynaptic specificity.

4.3.1 STP regulation at cell level: neuronal preference for specific interstimulus intervals (ISIs)

We reasoned that a simple readout for postsynaptic clustering of STP in thalamorecipient neurons was whether a neuron had a preference for specific ISIs. Uniform STP across the TC synaptic inputs to a given neuron would imply similar filtering of inputs and a net overall preference for a particular interval or range of

intervals. To examine this possibility we designed an experiment where a white noise current is injected through the recording electrode while stimulating the white matter with an extracellular bipolar electrode (Fig. 4.12), using 4 different patterns of stimulation (Materials and Methods, 3.3.1) characterized by different ISIs. We restricted the investigation of STP regulation to monosynaptic excitatory TC connections by eliminating the contribution of inhibitory currents through addition of DNDS to the intracellular solution (Materials and Methods, 3.4.1). White noise stimulation was used to bring the recorded neuron closer to action potential threshold and thus make it more susceptible to respond. Responses to each of the 4 synaptic stimulation patterns were recorded over 10 repetitions, with a different white noise pattern used for every repetition.

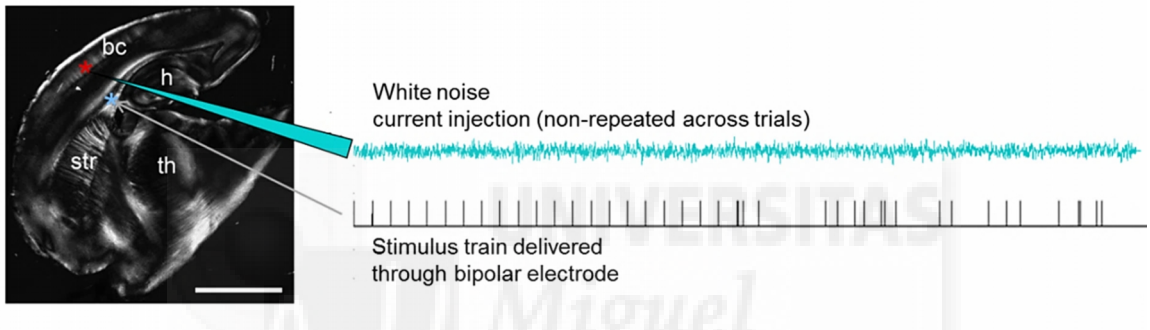

Figure 4.12: White noise current injection recording. Schematic of the recording configuration. A stimulation pattern (*Regular-irregular* in the figure) was delivered through a bipolar electrode placed in the white matter (illustrated by the grey arrow on the blue asterisk indicating the stimulation site), while a cell in layer 4 of the *bc* (red asterisk) was recorded injecting a different white noise current pattern (cyan trace) for each repetition. bc, Barrel cortex; th, thalamus; h, hippocampus; str, striatum. Scale bar, 1 mm.

This ensured that response preferences present across the 10 trails were due to the synaptic input pattern rather than any feature of the white noise stimulus. To assess the dependence of firing probability on the most recent ISI, for each recording we calculated the probability distribution of ISIs delivered through the synaptic extracellular stimulation electrode, and compared it to the distribution of ISIs present immediately before the recorded cell fired a spike (action potential). A difference between these ISI distributions would indicate that the neuron "preferred" the intervals over-represented in the spike-related distribution. Across the overall data set (n = 20), most neurons (n = 17) showed no clear specificity for certain ISIs; interestingly, a few (n = 3) displayed firing that occurred predominantly after ISIs that were shorter than expected, implying a preference for specific short ISIs (Fig. 4.13).

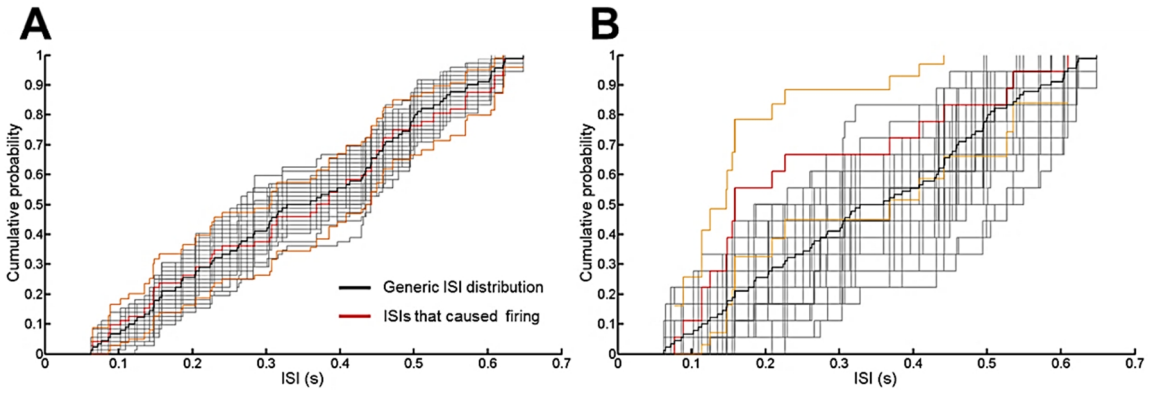

Figure 4.13: Neuronal preference for specific interstimulus intervals (ISIs).
Cumulative probability distribution of ISIs plotted against the ISIs present in the stimulation patterns. Black lines represent the generic ISIs distribution, red lines the ISIs distribution before the recorded cell fires a spike; grey and yellow lines represent the upper and lower 95% confidence bounds. **A**, Example plot for a neuron that displayed no specificity for any given ISIs. Note the similarity between the generic ISIs distribution (black line) and the ISIs distribution that caused firing (red line) for the cell. **B**, Example plot for a neuron that displayed clear specificity for shorter ISIs as compared to **A**, as evidenced by the difference between the two distributions.

However, in general, neurons seemed not to have a clear preference for specific ISIs. The relatively small number of neurons showing interval specificity could conceivably arise from a random assignment of particularly strongly facilitating or depressing TC inputs.

4.3.2 STP regulation at a cell-level: evaluation of post-synaptic clustering with non-minimal stimulation protocol

If a postsynaptic neuron has no cell-specific preference for a specific class of STP, the properties of different TC inputs onto the neuron will tend to be averaged together by postsynaptic integration. If so, synaptic stimulation with a strong magnitude (exciting multiple synapses onto a neuron) should evoke relatively similar STP in different neurons, because each cell would average together its multiple, distinct activated inputs. In contrast, stimulation with a weaker (minimal) magnitude, leading to excitation of only a very few synapses per neuron, would be expected to generate more diverse STP. Conversely, if postsynaptic neurons do regulate STP in cell-specific manner, then different synapses onto the same neuron will have similar dynamics, and stimulating with higher intensity should produce similar STP than stimulating with lower intensity:

thus, the diversity of STP evoked by high- and low-magnitude stimulation should not be different.

To distinguish between these possibilities we analyzed the behavior of different recordings when tested with minimal and non-minimal (larger magnitude) stimulation in the presence of DNDS to eliminate the inhibitory component. Facilitation index and TCS were again used as a measure of STP (Fig. 4.14). Comparison of STP under minimal and larger magnitude stimulation shows no difference between stimulation conditions for the two different populations ($p = 0.419$, 2-dimensional Kolmogorov-Smirnov two-sample test). There is thus no indication that postsynaptic cells average across their synaptic inputs. In both conditions STP heterogeneity is maintained. However, evoked responses did not linearly increase with the increasing amplitude of stimulation, probably reflecting a failure to recruit an increasing number of synapses, because of the limitations of the slice preparation.

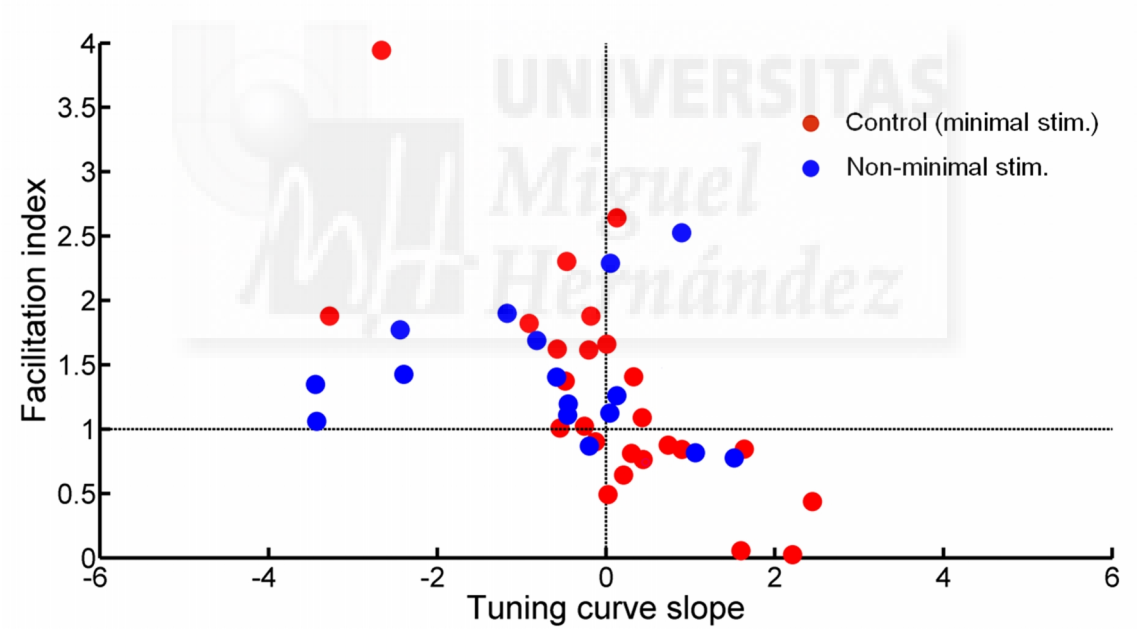

Figure 4.14: STP diversity across different stimulation conditions.
Facilitation index plotted against TCS for experiments conducted in standard conditions (minimal stim., red dots, n = 25) and strong stimulation magnitude (non-minimal stim., blue dots, n = 17) conditions, with DNDS in the intracellular solution to remove inhibitory contributions. STP heterogeneity was maintained across recordings.

Indeed, PSPs obtained with non-minimal stimulation might be low because of axon severing during the cutting procedure. For this reason, it seems not possible to lean towards a clear evidence for postsynaptic clustering.

5. Discussion

In the somatosensory system TC projections, although representing only a relatively small percentage of synaptic connections on cortical neurons, are a very important pathway responsible for the perception of sensory stimuli (Bruno, Sakmann, 2006). In the rodent neocortex, layer 4 neurons are the main target of lemniscal thalamic drive via monosynaptic connections. Consequently, the modulation of the dynamics of TC connections onto layer 4 plays a fundamental role in the transmission and processing of sensory information from the periphery. Neurons in the central nervous system are reached by several afferent synaptic connections, each of which is characterized by different inhibitory or facilitatory components. The interaction of the diverse components of STP can give rise to specific filtering functions useful for information processing (Fortune, Rose, 2001). For a long time synaptic plasticity has been only described considering the average properties of populations of a given type. However it has been pointed out that this description does not reflect the heterogeneity in behavior existing even at individual connections. TC projections have been considered in both *in vitro* (Gil et al., 1997, 1999; Stratford et al., 1996) and *in vivo* (Chung et al., 2002; Bruno, Sakmann, 2006) studies as classically depressing connections. Data recently published by our group (Diaz Quesada, Martini et al., 2014) have revealed that lemniscal TC connections respond with diverse STP when new stimuli arrive against a background of ongoing activity. In accordance with the literature, when stimulated from rest at periodical intervals, TC connections show a depressing behavior. However, as anticipated above, average synaptic properties are not sufficient to capture the variability in response found after a frequency change during ongoing stimulation. So, despite an average depressing behavior observed for TC projections when considered as a whole, important diversity within individual connections emerges around the mean.

In this project we have sought to describe mechanisms and specificity underlying STP heterogeneity. For the first part related to the mechanisms, our results show that STP variability emerges as a property of monosynaptic connections, without requiring a disynaptic inhibitory contribution. NMDA receptor blockade also had no effect on the distribution of STP, but extracellular calcium concentration did, suggesting a dependence on presynaptic mechanisms. While manipulation of kainate receptors did not lead to relevant modifications, modulation of adenosine receptor activity had an

important influence on STP by regulating neurotransmitter release. The effects took the form of a shift in TC connections' behavior while not eliminating the underlying variability. Finally, concerning specificity, our experiments aimed to find a regulation at the cell level provided weak evidence for postsynaptic clustering of STP properties.

5.1 Mechanisms underlying STP heterogeneity

5.1.1 STP variability has a monosynaptic locus

One possibility for STP diversity across synaptic connections could be represented by the contribution of the feedback inhibitory circuit characterizing the TC drive from the VPM to the barrel cortex (Fig. 4.1). Given this prominent role for inhibition in driving synaptic responses to sensory stimuli, we analyzed feedforward inhibitory dynamics to evaluate whether STP variability might be explained by differences in the rate of depression of the disynaptic inhibitory component of PSPs relative to the monosynaptic excitatory component. Our voltage clamp recordings showed connections with relatively strong excitation at the transition from periodic to irregular stimulation while others had a relatively strong inhibition at transition (Fig. 4.4). This variability suggests that "facilitating" and "depressing" projections could have different balance of excitation/inhibition dynamics. Despite showing differences in the dynamics of the disynaptic inhibitory component, this experiment was not conclusive to indicate a mechanism for STP diversity. Our results obtained blocking inhibition with the $GABA_A$ antagonist DNDS confirmed that STP diversity of TC synapses during ongoing stimulation can be explained by differences in the properties of monosynaptic excitatory connections (Fig. 4.3). Thus, while we showed that variation in the balance of excitation and disynaptic inhibition may enhance differences in STP dynamics across synapses, we also demonstrated that it is not necessary for STP diversity. This allowed us to restrict our mechanistic analysis of STP heterogeneity sources to the VPM to layer 4 monosynaptic excitatory pathway.

5.1.2 STP variability is likely caused by presynaptic factors

The next aim of our project was to try to define a synaptic locus for STP heterogeneity. Changes in synaptic strength during STP could be due to presynaptic alterations in neurotransmitter release or postsynaptic modifications in the properties of receptors. Mechanisms for STP may vary depending on the specific synapse in question: our current knowledge about synaptic transmission and STP is based to a large extent on the calyx of Held or hippocampal synapses, but it is not clear how the properties of these synapses generalize to others.

In our experimental model, TC synapses, earlier experiments from our group suggested that STP diversity arises predominantly from variation in presynaptic factors. Although short-term facilitating synapses could potentially arise from increased postsynaptic summation caused by broader PSPs, the earlier experiments found no correlation of facilitation index with PSP width, either for initial or ongoing responses (Diaz Quesada, Martini et al., 2014). Pharmacological blockade experiments investigated a possible participation of postsynaptic NMDA receptors in setting the type of STP. These found no apparent contribution, since NMDA receptor blockade did not alter evoked PSPs during ongoing stimulation.

On the presynaptic side, depletion of vesicles of the readily releasable pool, inactivation of release sites, and inactivation of presynaptic calcium channels can all contribute to synaptic depression. Conversely, local saturation of calcium buffers, facilitation of presynaptic calcium channels, and residual calcium-dependent processes can lead to synaptic facilitation (Zucker, Regehr, 2002; Fioravante, Regehr, 2011). We demonstrated that STP is affected by extracellular [Ca^{2+}]: recordings made using a low calcium concentration (1 mM) solution, more similar to physiological values in live animals, displayed significantly less depression than those in high calcium (2 mM) (Fig. 4.5). We then performed a further set of experiments to nail down the effect of extracellular [Ca^{2+}] on STP heterogeneity. We first evaluated the evoked PSPs under near-physiological calcium concentration (1 mM) and subsequently, while keeping the recording, raised the concentration to a much higher value (4 mM) in order to deplete faster the readily releasable pool and thus verify possible differences in the connections' response to ongoing stimulation. High [Ca^{2+}] significantly decreased the facilitation index and changed the distribution of values, not just its mean (Fig. 4.6). Taken

together, this evidence suggests, but falls short of demonstrating, a presynaptic mechanism.

The analysis of presynaptic mechanisms underlying STP has been a fundamental matter of study within the overall field of dynamic synaptic transmission. Since presynaptic vesicles are a limited resource, their depletion during ongoing activity can lead to suppression of the postsynaptic response. This concept led to the formalization of the first formal model of such a process, published by Liley and North (1953). Despite fitting well to some depressing synapses' behavior, it was demonstrated that other synapses show substantial deviations rendering it not ideal to predict STP dynamics. Therefore, release probability facilitation counteracting depression was added to extend the vesicle depletion model. Two related independently developed models (Tsodyks, Markram, 1997; Varela et al., 1997) for modeling information processing in neural networks are derived from the extension of depletion model. Both are based on three main concepts: the existence of a readily releasable pool (RRP) of vesicles that can be released depending on the presynaptic activity; a certain release probability per vesicle within the pool; and a set recovery rate for synaptic vesicles. Although these models have had great success, they are unable to explain the STP behavior present in our data simply with synaptic dynamics based on uniform resource depletion. Probably other mechanisms might be involved, including: probability of vesicle release and replenishment can accelerate after intensive stimulation, depending on an increase in intracellular calcium concentration (Garcia-Perez, Wesseling, 2008). Another mechanism could reside in the existence of different subsets of the RRP (Tsien, Alabi, 2012), one triggered by single action potential and termed "rapidly releasing", and a second called "slowly releasing", relatively reluctant to release in comparison to the first pool. Probably at TC synapses, like in other cerebral circuits (Wesseling, Lo, 2002), RRP consists of independent release sites that operate in parallel, each with a release probability that can be modulated independently. It would be important to formulate a sufficiently general, yet minimal model of STP that incorporates our findings, to better constrain mechanisms and explore functional consequences (e.g. Kandaswamy et al., 2010; Rotman et al., 2013).

5.1.3 Neuromodulators effect over STP

Multiple processes underlie STP, giving rise in each case to a combination of facilitation and depression in which synaptic strength is highly dependent on the details of the timing of synaptic activation (Tsodyks, Markram, 1997; Dittman et al., 2000). A wide range of STP regulators has been discovered over the past years. The properties and mechanisms of use-dependent STP can be modulated by extracellular molecules called neuromodulators. Neuromodulators might allow neuronal networks to select certain inputs for changes in synaptic efficacy. Our experiments indicate that the adenosine-receptor pathway seems to contribute to modulating TC synapse behavior. Interestingly, manipulation of adenosine receptor activation conserves STP diversity despite its effects on facilitation and TCS. It has been demonstrated that adenosine can reduce neuronal excitation activation of presynaptic adenosine receptors, which inhibit the release of glutamate by reducing calcium influx through inhibition of presynaptic Ca^{2+} channels (Lupica et al., 1992; Scanziani et al., 1992; Shen, Johnson, 2003; Dunwiddie, Masino, 2001). Our results support a role for adenosine in the modulation of TC STP dynamics, likely produced by binding to presynaptic receptors that probably produces a reduction in glutamate release. Results obtained in the presence of A1R-specific antagonists DPCPX and CPT suggest a fundamental role for this particular receptor family within the four adenosine receptors cloned so far (A1, A2A, A2B, and A3). It has been proposed that adenosine receptors present on TC terminals could provide an efficient method of limiting thalamic activation of the cortex (Fontanez, Porter, 2006). These authors confirmed that adenosine receptors provide a mechanism by which increased adenosine levels can directly reduce cortical excitability. Moreover, adenosine equally reduced TC inputs onto both inhibitory and excitatory neurons, suggesting that rising cortical adenosine levels would result in a global reduction in the impact of incoming sensory information. *In vivo* studies of adenosine application to the somatosensory cortex revealed an inhibition of potentials evoked by stimulation of the periphery (Petrescu, Haulica, 1983; Addae, Stone, 1988). Therefore, cortical adenosine levels have been demonstrated as responsible for regulating TC synapses and reducing the influence of sensory inputs on cortical activity.

Our data indicate that adenosine application to the extracellular bath produced an increase in facilitation index that could be explained by its effect on presynaptic adenosine receptors that inhibit the release of glutamate, thus decreasing tonic release

probability and modifying STP (Fig. 4.7). Interestingly, effects of the two specific A1R antagonists DPCPX and CPT were not observed on the facilitation index but on the TCS (Fig. 4.8). Specifically, blocking the A1R pathway caused an increase in TCS, rendering TC connections more responsive to long intervals.

5.2 Specificity of STP heterogeneity

STP properties can be regulated presynaptically or postsynaptically, implying an important difference in information processing at the cell level. We carried out experiments devoted to searching for postsynaptic clustering. It has been shown in different systems like the cochlear nucleus and excitatory synapses in the cerebellum (Yang, Xu-Friedman, 2009) that postsynaptic cells can coordinate the plasticity of their inputs. Following this rationale, we wondered whether this capacity could be found also at TC connections.

Our first result reveals that there is no evidence for a postsynaptic clustering of STP properties using a non-minimal stimulation protocol. Our stimulation approach was based on the idea that, if many fibers - instead of the lowest possible number activated by a minimal stimulation protocol - are stimulated at one time, then the dynamics of the synaptic inputs from multiple presynaptic cells would be averaged by the postsynaptic neuron. We reasoned that if a postsynaptic neuron shows a preference for a particular STP, this must be because different synapses onto the neuron have similar dynamics. In this case, high magnitude stimulation should produce similar STP than lower intensity stimulation, and different neurons will tend to show distinct (diverse) behavior. In contrast, a postsynaptic neuron that averages over synapses with different STP should not display sensitivity to specific intervals. In this case, non-minimal stimulation should evoke relatively similar STP in different neurons, leading to a reduction in STP variability compared to the minimal stimulation protocol. In practice, our recordings under non-minimal stimulation continued to show substantial heterogeneity (Fig. 4.14). However, this result is not straightforward to interpret, because although non-minimal TC fiber stimulation had considerably larger amplitude than minimal stimulation, postsynaptic responses were not significantly stronger, most likely due to axon severing during slice preparation. Thus, it is not clear that these experiments successfully

achieved the condition of sampling joint responses from a large number of synapses per neuron.

According to these findings, we designed a novel protocol combining minimal stimulation of TC synapses with noisy current stimulation of the membrane. Data from this experiment reveal that over 20 neurons recorded, only 3 were more responsive to short ISIs (Fig. 4.13). The few neurons that fired significantly more in response to short ISIs could have randomly received particularly strong facilitating or depressing TC inputs. Taken together, results fail to indicate clear evidence for postsynaptic clustering of STP properties, although the possibility cannot be ruled out either given that any single experimental approach will always be limited.

Similarity in STP properties could occur not only postsynaptically but presynaptically as well, i.e. with TC synapses from the same neurons sharing common dynamics. To analyze possible specificity of STP behavior in excitatory connections of TC neurons we have begun pilot imaging experiments with the glutamate sensor iGluSnFR (Marvin et al., 2013). This is a particularly sensitive, photostable and fast reporter that can putatively report excitatory release in single synapses. We are infecting the VB thalamus of mice with viral delivery of AAV.hSynapsin.iGluSnFR. After viral expression, cells from the VB thalamus reaching layer 4 neurons in the somatosensory cortex will be imaged under two photon microscopy as glutamate is released from the terminals of the presynaptic cells in response to stimulation. Whole cell recordings will serve as a readout of postsynaptic responses.

In conclusion, we have explored STP variability across TC synapses and demonstrated that monosynaptic excitatory lemniscal TC connections onto layer 4 do not behave uniformly during ongoing stimulation; instead, synapses show distinct responses to particular stimulation intervals. The neuromodulator adenosine can alter STP properties. STP diversity can enrich information transmission in the TC pathway. It remains an open question whether STP is specifically regulated at the presynaptic or postsynaptic cell level. Addressing this issue will help us to understand how sensory information is encoded in the thalamus and then decoded and transformed in the cortex.

6. Conclusions

1. Lemniscal TC connections respond with diverse STP when new stimuli arrive against a background of ongoing activity.

2. STP variability emerges as a property of monosynaptic excitatory connections, without requiring a disynaptic inhibitory contribution.

3. Although it is not necessary for STP diversity, variation in the balance of excitation and disynaptic inhibition may enhance differences in STP dynamics across synapses.

4. STP variability is likely caused by presynaptic factors: extracellular [Ca2+] has a significant influence on the distribution of STP. On the contrary, postsynaptic NMDA receptors display no apparent contribution in setting the type of STP.

5. Modulation of adenosine receptor activity has an important influence on STP by regulating neurotransmitter release: it induces a shift in TC connections' behavior while not eliminating the underlying variability.

6. Modulation of kainate receptor activity does not lead to relevant modifications to STP variability.

7. Results concerning the specificity of STP heterogeneity display no clear evidence for postsynaptic clustering of STP properties.

7. References

Abbott LF (1997) Synaptic Depression and Cortical Gain Control. Science, 275(5297), 221–224.

Abbott LF, Regehr WG (2004) Synaptic computation, review article. Nature 431, 796-803.

Abbott LF, Varela JA, Sen K, Nelson SB (1997) Synaptic depression and cortical gain control. Science 275(5297):220-4.

Addae JI, Stone TW (1988) Purine receptors and kynurenic acid modulate the somatosensory evoked potential in rat cerebral cortex. Electroencephalogr Clin Neurophysiol 69:186–189.

Agmon A, Connnors BW (1991) Thalamocortical responses of mouse somatosensory (barrel) cortex in vitro. Neuroscience 41(2-3):365-79.

Allen C, Stevens CF (1994) An evaluation of causes for unreliability of synaptic transmission. Proceedings of the National Academy of Sciences of the United States of America, 91(10), 10380–10383.

Beierlein M, Gibson JR, Connors BW (2003) Two Dynamically Distinct Inhibitory Networks in Layer 4 of the Neocortex. Journal of Neurophysiology 90(5), 2987-3000.

Benshalom G, White J (1986) Quantification of thalamocortical synapses with spiny stellate neurons in layer IV of mouse somatosensory cortex. J. Comp. Neurol. 253, 303.

Bettler B, Mulle C (1995) Review: neurotransmitter receptors. II. AMPA and kainate receptors. Neuropharmacology. (2):123-39. Review.

Blackman AV, Abrahamsson T, Costa RP, Lalanne T., Sjöström PJ (2013) Target-cell-specific short-term plasticity in local circuits. Frontiers in Synaptic Neuroscience, 5(12), 11.

Bliss TV, Collingridge GL (1993) A synaptic model of memory: long-term potentiation in the hippocampus. Nature 361 (6407): 31–39.

Borgdorff AJ, Poulet JF, Petersen CC (2007) Facilitating sensory responses in developing mouse somatosensory barrel cortex. J Neurophysiol. 97:2992–3003.

Boudreau CE, Ferster D (2005) Short-term depression in thalamocortical synapses of cat primary visual cortex. J Neurosci. 25:7179 –7190.

Bozdagi O, Valcin M, Poskanzer K, Tanaka H, Benson DL (2004) Temporally distinct demands for classic cadherins in synapse formation and maturation, 27, 509–521.

Carandini, M, Ferster, D (1997) A tonic hyperpolarization underlying contrast adaptation in cat visual cortex. Science 276 (5314): 949–52.

Castro-Alamancos MA (2004) Absence of rapid sensory adaptation in neocortex during information processing states. Neuron. 41(3):455-64.

Castro-Alamancos MA, Oldford E (2002) Cortical sensory suppression during arousal is due to the activity-dependent depression of thalamocortical synapses. J Physiol. 541:319–331.

Chittajallu R, Vignes M, Dev KK, Barnes JM, Collingridge GL, Henley JM (1996) Regulation of glutamate release by presynaptic kainate receptors in the hippocampus. Nature. 379(6560):78-81.

Chung S, Li X, Nelson SB (2002) Short-term depression at thalamocortical synapses contributes to rapid adaptation of cortical sensory responses in vivo. Neuron. 34(3):437-46.

Chung S, Li X, Nelson SB (2002) Short-term depression at thalamocortical synapses contributes to rapid adaptation of cortical sensory responses in vivo. Neuron, 34: 437-446.

Covic EN, Sherman SM (2011) Synaptic properties of connections between the primary and secondary auditory cortices in mice. Cerebral Cortex, 21(11), 2425–2441.

Crair MC, Malenka RC (1995) A critical period for long-term potentiation at thalamocortical synapses. Nature 375(6529):325-8.

Davies CH, Davies SN, Collingridge GL (1990) Paired-pulse depression of monosynaptic GABA-mediated inhibitory postsynaptic responses in rat hippocampus. J. Physiol. 424:513–31.

Dean C, Dresbach T (2006) Neuroligins and neurexins: linking cell adhesion, synapse formation and cognitive function. TrendsNeurosci. 29, 21–29.

Deschenes, Urbain (2009) Scholarpedia, 4(5):7454.

Díaz-Quesada M, Maravall M (2008) Intrinsic mechanisms for adaptive gain rescaling in barrel cortex. J Neurosci 28:696 –710.

Díaz-Quesada M, Martini, FJ, Ferrati G, Bureau I, Maravall M (2014) Diverse thalamocortical short-term plasticity elicited by ongoing stimulation. J Neurosci 34(2), 515–26.

Dittman JS, Kreitzer AC, Regehr WG (2000) Interplay between facilitation, depression, and residual calcium at three presynaptic terminals. J Neurosci. 20(4):1374-85.

Dittman JS, Regehr WG (1998) Calcium dependence and recovery kinetics of presynaptic depression at the climbing fiber to Purkinje cell synapse. J Neurosci. 18(16):6147-62.

Dobrunz LE, Stevens CF (1999) Response of hippocampal synapses to natural stimulation patterns. Neuron, 22(1), 157–66.

Dobrunz LE, Stevens CF (1997) Heterogeneity of release probability, facilitation, and depletion at central synapses. Neuron. 18(6):995-1008.

Drake CT, Terman GW, Simmons ML, Milner TA, Kunkel DD (1994) Dynorphin opioids present in dentate granule cells may function as retrograde inhibitory neurotransmitters. J. Neurosci. 14:3736–50.

Dudek SM, Friedlander MJ (1996) Intracellular blockade of inhibitory synaptic responses in visual cortical layer IV neurons. Journal of Neurophysiology 75(5), 2167-2173.

Dunwiddie TV, Masino SA (2001) The role and regulation of adenosine in the central nervous system. Annu Rev Neurosci 24:31-55.

Feigenspan A, Gustincich S, Bean BP, Raviola E (1998) Spontaneous activity of solitary dopaminergic cells of the retina. J. Neurosci. 18:6776–89.

Fioravante D, Regehr WG (2011). Short-term forms of presynaptic plasticity. Curr Opin Neurobiol; 21:269-74

Fontanez DE, Portrer JT (2006) Adenosine A1 Receptors decrease thalamic excitation of inhibitory and excitatory neurons in the barrel cortex. Neuroscience 137:1177–1184.

Fortune ES, Rose GJ (2001) Short-term synaptic plasticity as a temporal filter. Trends Neurosci. 24(7):381-5.

Foster KA, Kreitzer AC, Regehr WG (2002) Interaction of postsynaptic receptor saturation with presynaptic mechanisms produces a reliable synapse. Neuron 36(6):1115-26.

Frerking M, Schmitz D, Zhou Q, Johansen J, Nicoll RA (2001) Kainate receptors depress excitatory synaptic transmission at CA3-CA1 synapses in the hippocampus via a direct presynaptic action. J. Neurosci. 21, 2958–2966.

Gabernet L, Jadhav SP, Feldman DE, Carandini M, Scanziani M (2005) Somatosensory integration controlled by dynamic thalamocortical feed-forward inhibition. Neuron, 48(2), 315–327.

Garcia-Perez E, Wesseling JF (2008) Augmentation controls the fast rebound from depression at excitatory hippocampal synapses. Journal of Neurophysiology, 99(2008), 1770–1786.

Gil Z, Connors BW, Amitai Y (1997) Differential regulation of neocortical synapses by neuromodulators and activity. Neuron 19(3):679-686.

Gil Z, Connors BW, Amitai Y (1999) Efficacy of thalamocortical and intracortical synaptic connections: quanta, innervation, and reliability. Neuron 23(2):385-397.

Gundlfinger A, Bischofberger J, Johenning FW, Torvinen M, Schmitz D, Breustedt J (2007) Adenosine modulates transmission at the hippocampal mossy fibre synapse via direct inhibition of presynaptic calcium channels. J Physiol 582:263–277 263.

Hutson KA, Masterton RB (1986) The sensory contribution of a single vibrissa's cortical barrel. J Neurophysiol (56)1196–1223.

Isaac JT, Mellor J, Hurtado D, Roche, KW (2004) Kainate receptor trafficking: physiological roles and molecular mechanisms. Pharmacol. Ther. 104, 163e172.

Isaacson JS, Solis JM, Nicoll RA (1993) Local and diffuse synaptic actions of GABA in the hippocampus. Neuron 10:165–75.

Jadhav SP, Feldman DE (2010) Texture coding in the whisker system. Current Opinion in Neurobiology, 20(3), 313–8.

Jenks RA, Vaziri A, Boloori AR, Stanley GB (2010) Self-motion and the shaping of sensory signals J Neurophysiol. (103)2195–2207.

Jiang L, Xu J, Nedergaard M, Kang J (2001) A kainate receptor increases the efficacy of GABAergic synapses. Neuron 30, 503e513.

Johansen TH, Drejer J, Wätjen F, Nielsen EØ (1993) A novel non-NMDA receptor antagonist shows selective displacement of low-affinity [3H]kainate binding. Eur. J. 15; 246(3):195-204.

Kandaswamy U, Deng PY, Stevens CF, Klyachko VA (2010) The role of presynaptic dynamics in processing of natural spike trains in hippocampal synapses. J. Neurosci. Nov 24;30(47):15904-14.

Katz B (1969) The Release of Neural Transmitter Substance. Liverpool, UK: University Press.

Kerr JN, de Kock CP, Greenberg DS, Bruno RM, Sakmann B, Helmchen F (2007) Spatial organization of neuronal population responses in layer 2/3 of rat barrel cortex. J Neurosci. Nov 27(48):13316-28.

Kidd FL, Coumis U, Collingridge GL, Crabtree JW, Isaac JT (2002) A presynaptic. Kainate receptor is involved in regulating the dynamic properties of thalamocortical synapses during development. Neuron 34, 635e646.

Kidd, FL, Isaac JT (1999) Developmental and activity-dependent regulation of kainate receptors at thalamocortical synapses. Nature 400, 569–573.

Klyachko VA, Stevens CF (2006) Excitatory and feed-forward inhibitory hippocampal synapses work synergistically as an adaptive filter of natural spike trains. PLoS Biology, 4(7), 1187–1200.

Knutsen PM, Pietr M, Ahissar E (2006) Haptic object localization in the vibrissal system: behavior and performance. J Neurosci, (26)8451–8464.

Kombian SB, Mouginot D, Pittman QJ (1997) Dendritically released peptides act as retrograde modulators of afferent excitation in the supraoptic nucleus in vitro. Neuron. 19(4):903-12.

Kreitzer AC, Regehr WG (2001) Retrograde inhibition of presynaptic calcium influx by endogenous cannabinoids at excitatory synapses onto Purkinje cells. Neuron 29:717–27.

Krupa DJ, Matell MS, Brisben AJ, Oliveira JM, Nicolelis MA (2001) Behavioral properties of the trigeminal somatosensory system in rats performing whisker-dependent tactile discriminations. J Neurosci. (21) 5752–5763.

Kullmann DM (2001) Presynaptic kainate receptors in the hippocampus: slowly emerging from obscurity. Neuron 20;32(4):561-4.

Lak A, Arabzadeh E, Diamond ME (2008) Enhanced response of neurons in rat somatosensory cortex to stimuli containing temporal noise. Cereb Cortex. (5):1085-93.

Lak A, Arabzadeh E, Harris JA, Diamond ME (2010) Correlated physiological and perceptual effects of noise in a tactile stimulus. Proc Natl Acad Sci U S A. (17):7981-6.

Land PW, Kandler K (2002) Somatotopic organization of rat thalamocortical slices. J Neurosci Methods 15;119(1):15-21.

Lauri SE, Vesikansa A, Segerstråle M, Collingridge GL, Isaac JT, Taira T (2006) Functional maturation of CA1 synapses involves activity-dependent loss of tonic kainate receptor-mediated inhibition of glutamate release. Neuron. 50(3):415-29.

Lerma J (2003) Roles and rules of Kainate receptors in synaptic transmission. Nat Rev Neurosci. 4(6):481-9514.

Lerma J, Paternain AV, Rodriguez-Moreno A, Lopez-Garcia JC (2001) Molecular physiology of kainate receptors. Physiol. Rev. 81, 971e998.

Liley AW, North KA (1953) An electrical investigation of effects of repetitive stimulation on mammalian neuromuscular junction. J. Neurophysiol.16,509–527.

Losonczy A, Zhang L, Shigemoto R, Somogyi P, Nusser Z (2002) Cell type dependence and variability in the short-term plasticity of EPSCs in identified mouse hippocampal interneurons. J Physiol 542:193–210.

Lübke J, Egger V, Sakmann B, Feldmeyer D (2000) Columnar organization of dendrites and axons of single and synaptically coupled excitatory spiny neurons in layer 4 of the rat barrel cortex. J Neurosci 20(14), 5300–5311.

Lupica CR, Proctor WR, Dunwiddie TV (1992) Presynaptic inhibition of excitatory synaptic transmission by adenosine in rat hippocampus: analysis of unitary EPSP variance measured by whole-cell recording. J Neurosci 12:3753-3764.

Markram H, Wang Y, Tsodyks M (1998) Differential signaling via the same axon of neocortical pyramidal neurons. Proc Natl Acad Sci U S A. 95(9):5323-8.

Marvin JS, Borghuis BG, Tian L, Cichon J, Harnett MT, Akerboom J, Looger LL (2013) An optimized fluorescent probe for visualizing glutamate neurotransmission, Nature Methods 10(2).

McCormick DA, Connors BW, Lighthall JW, Prince DA (1985) Comparative electrophysiology of pyramidal and sparsely spiny stellate neurons of the neocortex. Journal of Neurophysiology, 54(4), 782–806.

Moore KA, Nicoll RA, Schmitz D (2003) Adenosine gates synaptic plasticity at hippocampal mossy fiber synapses. Proc Natl Acad Sci U S A. 100(24):14397-402.

Mulle C, Sailer A, Pérez-Otaño I, Dickinson-Anson H, Castillo PE, Bureau I, Maron C, Gage FH, Mann JR, Bettler B, Heinemann SF (1998) Altered synaptic physiology and reduced susceptibility to kainate-induced seizures in GluR6-deficient mice. Nature. 392(6676):601-5.

Mulle C, Sailer A, Swanson GT, Brana C, O'Gorman S, Bettler B, Heinemann SF (2000) Subunit composition of kainate receptors in hippocampal interneurons. Neuron.28(2):475-84.

Murthy VN, Sejnowski TJ, Stevens CF (1997) Heterogeneous release properties of visualized individual hippocampal synapses. Neuron 18:599–612.

O'Connor DH, Peron SP, Huber D, Svoboda K (2010) Neural activity in barrel cortex underlying vibrissa-based object localization in mice. Neuron 67(6):1048-61.

Petersen RS, Brambilla M, Bale MR, Alenda A, Panzeri S, Montemurro MA, Maravall M (2008) Diverse and temporally precise kinetic feature selectivity in the VPm thalamic nucleus. Neuron 60:890–903.

Petrescu G, Haulica I (1983) Preliminary data concerning adenosine action upon the evoked potential after electrical stimulation of the vibrissal follicles in the adult rat. Physiologie 20:229–233.

Pologruto TA, Sabatini BL, Svoboda K (2003) ScanImage: flexible software for operating laser scanning microscopes. Biomed Eng Online 2:13.

Raastad M, Storm JF, Andersen P (1992) Putative Single Quantum and Single Fibre Excitatory Postsynaptic Currents Show Similar Amplitude Range and Variability in Rat Hippocampal Slice. Eur J Neurosci 4(1):113-117.

Reig R, Gallego R, Nowak LG, Sanchez-Vives MV (2006) Impact of cortical network activity on short-term synaptic depression. Cereb Cortex 16:688–695.

Reyes A, Lujan R, Rozov A, Burnashev N, Somogyi P, Sakmann B (1998) Target-cell-specific facilitation and depression in neocortical circuits. Nat Neurosci 1:279 – 285.

Reyes A, Sakmann B (1999) Developmental switch in the short-term modification of unitary EPSPs evoked in layer 2/3 and layer 5 pyramidal neurons of rat neocortex. J Neurosci 19:3827-3835.

Rose HJ, Metherate R (2001) Thalamic stimulation largely elicits orthodromic, rather than antidromic, cortical activation in an auditory thalamocortical slice. Neuroscience 106:331–340.

Rosenmund C, Clements JD, Westbrook GL (1993) Nonuniform probability of glutamate release at a hippocampal synapse. Science 262(5134):754-757.

Rotman Z, Klyachko VA (2013) Role of synaptic dynamics and heterogeneity in neuronal learning of temporal code. J Neurophysiol. 2013 Nov;110(10):2275-86.

Sakmann B, Neher E (1984) Patch clamp techniques for studying ionic channels in excitable membranes. Annual Reviews Physiology 46: 455–472.

Sato TR, Gray NW, Mainen ZF, Svoboda K (2007) The functional microarchitecture of the mouse barrel cortex. PLoS Biol. 5(7):e189.

Scanziani M, Capogna M, Gahwiler BH, Thompson SM (1992) Presynaptic inhibition of miniature excitatory synaptic currents by baclofen and adenosine in the hippocampus. Neuron 9:919-927.

Shen KZ, Johnson SW (2003) Presynaptic inhibition of synaptic transmission by adenosine in rat subthalamic nucleus in vitro. Neuroscience 116:99-106.

Stratford KJ, Tarczy-Hornoch K, Martin KA, Bannister NJ, Jack JJ (1996) Excitatory synaptic inputs to spiny stellate cells in cat visual cortex. Nature. 382(6588):258-61.

Thomson AM, Lamy C (2007) Functional maps of neocortical local circuitry. Front Neurosci 1:19–42.

Tsodyks MV, Markram H (1997) The neural code between neocortical pyramidal neurons depends on neurotransmitter release probability. Proc Natl Acad Sci U S A 94(2):719-23.

Urbain N, Deschênes M (2007) A new thalamic pathway of vibrissal information modulated by the motor cortex. J. Neurosci. 27, 12407–12412.

Varela JA, Sen K, Gibson J, Fost J, Abbott LF, Nelson SB (1997) A quantitative description of short-term plasticity at excitatory synapses in layer 2/3 of rat primary visual cortex. J. Neurosci. 17, 7926–7940.

Wilent WB, Contreras D (2005) Dynamics of excitation and inhibition underlying stimulus selectivity in rat somatosensory cortex. Nat Neurosci. 8(10):1364-70.

Wilson RI, Nicoll RA (2002) Endocannabinoid signaling in the brain. Science 296, 678–682.

Xu-Friedman MA, Regehr WG (2004) Structural contributions to short-term synaptic plasticity. Physiol Rev 84: 69–85.

Yang H, Xu-Friedman MA (2012) Emergence of Coordinated Plasticity in the Cochlear Nucleus and Cerebellum. The Journal of Neuroscience, 32(23):7862–7868.

Yu C, Derdikman D, Haidarliu S, Ahissar E (2006) Parallel thalamic pathways for whisking and touch signals in the rat. PLoS Biology, 4(5), e124.

Zucker RS, Regehr WG (2002) Short-term synaptic plasticity. Annual Review of Physiology, 64, 355–405.

Zuo Y, Perkon I, Diamond ME (2011) Whisking and whisker kinematics during a texture classification task. Philos Trans R Soc Lond B Biol Sci, (366)3058–3069.